Pan African University
Institute of Water
and Energy Sciences

PAN-AFRICAN UNIVERSITY
INSTITUTE FOR WATER AND ENERGY SCIENCES
(including CLIMATE CHANGE)

Master Dissertation

Submitted in partial fulfillment of the requirements for the Master degree in

[WATER ENGINERING]

Presented by

Victo NABUNYA

Simulation of impacts of land-use and land cover changes on water balance in Oued Fez basin (Morocco)

Defended on 21/09/2020 Before the Following Committee:

Chair	**Abdelkader Douaoui**	**Prof.**	**University of Tipaza**
Supervisor	**Abdelkader El Garouani**	**Prof.**	**USMBA (FST-Fez)**
External Examiner	**John Gathenya**	**Prof.**	**JKUAT (Kenya)**
Internal Examiner	**Yacine Djebbar**	**Dr.**	**University of Souk Ahrass**

Declaration

I declare that this thesis is my personal work, and all the information, material and results from other works presented here, have been fully cited and referenced in accordance with the research ethics.

Signature 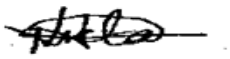 Date: **August 07, 2020**

Victo Nabunya

Recommendation

This thesis has been prepared under my close supervision and is the candidate's original work. It is therefore presented for examination under my approval.

Supervisor

Signature: 

Name: **Prof Abdelkader El Garouani** Date: **August 06, 2020**

Dedication

I dedicate this dissertation to my parents, Kabuye Godfrey and Kobusingye Faridah for their constant support and prayers.

Acknowledgement

My sincere gratitude also goes to the African Union Commission (AUC) and the German Ministry of Foreign Affairs through the Pan African University Institute of Water and Energy Sciences (PAUWES), for the scholarship award they offered me, I also the Algerian Government for facilitating my stay in Algeria. I wish to thank the PAUWES fraternity for their valuable academic support and guidance through the entire period of my masters' study.

I extend my gratitude to Prof Abdelkader El Garouani my supervisor for the continued guidance through my masters' research and the support he offered me during my stay in Morocco.

I would also like to express my sincere gratitude to:

- The Jury members: Prof. Abdelkader El Garouani , Prof. Abdelkader Douaoui the chairperson, Prof. John Gathenya the external examiner, and Dr Yacine Djebbar the internal examiner.
- The Laboratory of Functional Ecology and Environmental Engineering of the Faculty of Sciences and Techniques of Fez (Morocco).

Special thanks to Prof Gathenya John Mwangi, who consistently helped me through my master thesis research, particularly the use of SWAT model and provided his technical advice.

Finally, I thank my family, friends and the PAUWES class of 2020 for their support and contributions towards my study period in all their capacities.

Abstract

Land-use and land cover changes have great impacts on both the hydrology and water balance in a watershed and therefore evaluation of these impacts can greatly help in efficient water resources management. The Oued Fez basin has undergone severe land-use changes in the past 30 years (1988-2018). The objective of this research was to assess the impacts of land use changes in the Oued Fez basin, water balance using the Soil and Water Assessment Tool (SWAT) model, remote sensing and GIS techniques. The changes in the basin's water balance are attribute to the changes in land-use and land cover. The assessment was conducted using two land cover maps, 1988 and 2018 respectively and climatic data for period (1988-2018). The calibration was done using 17 random points of observed stream flow data collected over the period 2009-2011, while no data was available for validation. Over the 30 year period, rangelands drastically reduced by (333.62%), big increases were observed for urban (72.71%), arboriculture (90.43), water (36.85%), and irrigated agriculture (33. 78%). The CN2 and ESCO were adjusted to obtain results of long-term catchment water balance and monthly streamflow that matched the observations. The impacts of land-use change on the long term annual average water balance indicated an increase in the; total water yield by 1.20%, and surface runoff by 5.10%, reductions were also noted for: ET by 0.44%, lateral flow by 1.49%, ground water in shallow aquifer by 10.28%, and groundwater deep aquifer by 10.37%.

Statistical tools including NSE, PBIAS and R^2 were used to evaluate the model observed performance. NSE value of -2.45, PBIAS of 9.70 and R^2 of 0.42 were obtained during the calibration period, and the performance evaluation indicated a model underestimation during the calibration period. The simulation results also indicate an influence of land-use changes, on the hydrological water balance and streamflow. Generally, the model performance was unsatisfactory and this is due to insufficient data for calibration. If all uncertainties are addressed the model would give reasonable hydrologic simulations.

Key words: Land-use change, water balance, SWAT model, remote sensing, GIS, Oued Fez basin, Morocco.

Résumé

Les changements d'utilisation et de couverture des terres ont de grandes répercussions sur l'hydrologie et le bilan hydrique d'un bassin hydrographique et, par conséquent, l'évaluation de ces répercussions peut grandement contribuer à une gestion efficace des ressources en eau. Le bassin de l'Oued Fès a subi de graves changements d'utilisation des terres au cours des 30 dernières années (1988-2018). L'objectif de cette recherche était d'évaluer les impacts des changements d'utilisation des terres dans le bassin de l'Oued Fez, le bilan hydrique en utilisant le modèle SWAT (Soil and Water Assessment Tool), la télédétection et les techniques SIG. Les changements dans le bilan hydrique du bassin sont attribués aux changements dans l'utilisation des terres et la couverture des terres. L'évaluation a été réalisée à l'aide de deux cartes de l'occupation des sols, respectivement de 1988 et 2018, et de données climatiques pour la période (1988-2018). Le calibrage a été effectué en utilisant 17 points aléatoires de données sur le débit des cours d'eau observés, collectées sur la période 2009-2011, alors qu'aucune donnée n'était disponible pour validation. Sur la période de 30 ans, les parcours ont été réduits de manière drastique (333,62%), de fortes augmentations ont été observées pour les zones urbaines (72,71%), l'arboriculture (90,43), l'eau (36,85%) et l'agriculture irriguée (33,78%). La CN2 et l'ESCO ont été ajustées pour obtenir les résultats du bilan hydrique à long terme du bassin versant et du débit mensuel qui correspondaient aux observations. Les impacts du changement d'utilisation des terres sur le bilan hydrique annuel moyen à long terme ont indiqué une augmentation du rendement total en eau de 1,20 % et du ruissellement de surface de 5,10 %, des réductions ont également été notées : ET de 0,44 %, l'écoulement latéral de 1,49 %, les eaux souterraines des aquifères peu profonds de 10,28 % et les eaux souterraines des aquifères profonds de 10,37 %.

Des outils statistiques, notamment NSE, PBIAS et R2, ont été utilisés pour évaluer les performances observées du modèle. Une valeur NSE de -2,45, PBIAS de 9,70 et R2 de 0,42 ont été obtenues pendant la période de calibration, et l'évaluation des performances a indiqué une sous-estimation du modèle pendant la période de calibration. Les résultats de la simulation indiquent également une influence des changements d'utilisation des terres, sur le bilan hydrologique et le débit des cours d'eau. En général, la performance du modèle était insatisfaisante et cela est dû à l'insuffisance des données pour le calibrage. Si toutes les incertitudes sont prises en compte, le modèle donnerait des simulations hydrologiques raisonnables.

Mots clés : Changement d'utilisation du sol, bilan hydrologique, modèle SWAT, télédétection, SIG, bassin de l'Oued Fès, Maroc.

Table of Contents

Declaration i

Dedication ii

Acknowledgement iii

Abstract iv

Résumé v

List of Acronyms x

List of Tables xi

List of Figures xii

CHAPTER ONE 1

INTRODUCTION 1

1.1 Background 1

1.2 Problem statement 2

1.3 Objectives 3

1.4 Research questions 3

1.5 Justification 3

1.6 Scope of the study 4

1.7 Thesis Outline 4

CHAPTER TWO 5

LITERATURE REVIEW 5

2 Land-use / land cover changes 5

2.1 GIS and remote sensing use in monitoring land-use and land cover changes 5

2.2 Impacts of land-use changes on hydrology 6

2.3 Impacts of Climate Change on hydrology 6

2.4 Basin water balance 7

2.5 Hydrological modelling 7

2.6 Types of models 8

2.6.1 Empirical models 8
2.6.2 Conceptual models 8
2.6.3 Physically based models 9
2.6.4 Lumped models. 9
2.6.5 Distributed models 9
2.6.6 Semi distributed model 10
2.7 Description of selected hydrological models. 10
2.7.1 HBV model (Hydrologiska Byrans Vattenavdelning model) 10
2.7.2 TOPMODEL 11
2.7.3 Water Balance Model (WetSpass) 11
2.7.4 SWAT model 12
CHAPTER THREE 16
METHODOLOGY 16
3 Description of study area 16
3.1.1 Topography of the watershed 16
3.1.2 Population 17
3.1.3 Climatic conditions 18
3.1.4 Hydrology 20
3.1.5 Aquifer recharge 22
3.1.6 Geology of Oued Fez watershed 22
3.1.7 Economic Activities 23
3.2 Land use classification for 1988 and 2018. 24
3.2.1 Land use/cover change detection and analysis 25
3.2.2 Accuracy assessment of classification 25
3.3 Data preparation for hydrological modelling 26
3.3.1 Digital Elevation Model (DEM) 28
3.3.2 Weather data 28

3.3.3 Soil data 30
3.3.4 Land use and land cover 31
3.4 Streamflow data 32
3.5 Determination of water balance components under different land use 33
3.5.1 Watershed delineation and HRU analysis 34
3.5.2 Writing input tables 35
3.6 Model simulation, calibration and validation 36
3.7 Performance evaluation for SWAT model 39
CHAPTER FOUR 42
RESULTS AND DISCUSSIONS 42
4 Land use Land cover analysis 42
4.1.1 Accuracy assessment and validation 43
4.1.2 Land use/cover change detection and analysis 46
4.2 Model simulation 47
4.2.1 Calibration and validation 47
4.3 Impacts of LULC on water balance 48
4.4 Evaluation of model efficiency 51
Conclusion 52
Recommendations 53

List of Acronyms

ABHS	Sebou Hydraulic Basin Agency
DEM	Digital Elevation Model
CN	Curve Number
ET	Actual evapotranspiration
ETM	Enhanced Thematic Mapper
HRU	Hydrologic Response Unit
HYDGRP	Hydrologic soil group
LULC	Land use Land cover
MLC	Maximum likely classification
NSE	Nash-Sutcliffe Efficiency
PBIAS	Percent bias
PCP	Precipitation
PET	Potential evapotranspiration
RS	Remote sensing
SURF Q	Surface runoff
SWAT	Soil and Water Assessment Tool
TM	Thematic Mapper
TWYLD	Total water yield
USGS	United State Geological Survey

List of Tables

Table 3.1: Population of rural and urban households in Morocco, projecting Fez city (HCP, 2015) 17

Table 3.2: Rating of kappa statistics. 26

Table 3.3: Input parameters for SWAT model. 27

Table 3.4: FAO User soil 31

Table 3.5: Showing the SWAT land use codes. 32

Table 3.6: Stream flow data for the period 2009-2011. 32

Table 3.7: Most sensitive SWAT parameters. 37

Table 3.8: Statistical criterion. 41

Table 4.1: Error matrix accuracy assessment for 1988 45

Table 4.2: Error matrix accuracy assessment for 2018. 45

Table 4.3: Area of land use 1988 and 2018. 46

Table 4.4: long term annual average water balance components for land use simulations, with climate data (1988-2018) and Land-use data for 1988 & 2018. 48

Table 4.5: Average monthly basin values for the period (1988-2018) and LULC 1988. 50

Table 4.6: Average monthly basin values for the period (1988-2018) and LULC 2018. 50

List of Figures

Figure 3.1: Location of Oued Fez basin.....17

Figure 3.2: Rural and urban population growth in Morocco 18

Figure 3.3: Average monthly precipitation of Fez region at Fez-Saiss Station. 19

Figure 3.4: Average maximum and minimum monthly temperatures of Fez region at Fez-Saiss Station. 19

Figure 3.5: Average monthly potential evapotranspiration of Fez region at Fez Saiss Station. 20

Figure 3.6: Showing the aquifers in Saïss plain.....22

Figure 3.7: Ground truth points in google earth 26

Figure 3.8: Graphical representation of methodology. 28

Figure 3.9: Digital Elevation model.....30

Figure 3.10: Soil map for the watershed.....33

Figure 3.11: Sub basins in the watershed.....35

Figure 3.12: Slope map for the basin. 38

Figure 4.1: Land-use classification map for 2018 42

Figure 4.2: Land use classification map for 1988. 43

Figure 4.3: Variation in land-use between 1988 and 2018. 47

Figure 4.4: daily simulated and observed flow values during calibration period (2009-2011). 48

Figure 4.5: Scatter plot for observed versus simulated flow during calibration period. 51

CHAPTER ONE

INTRODUCTION

1.1 Background

Land-use and land cover changes impact the soil distribution and topography, often leading to water balance components changes (Awotwi, 2009). According to Bai *et al* (2015), for efficient management of water resources, assessment and evaluation of the effects of land-use change on the watershed water balance components is very crucial. Previous studies in Morocco have been associated to impacts of land use on sediment yield, water quality and run off but limited studies assessing impacts on water balance components of unconfined aquifers (Briak et al., 2016; Chadli et al 2016). Land use change is a very important factor considered in global change studies (Gamo, et al., 2013; Loveland et al., 2000; Tsarouchi et al., 2014).Land use describes exploitation of land resources by humans (Collins et al., 2002). Nonetheless, the impact of future land-use changes on the groundwater system has not been investigated extensively (Yun et al., 2011). Various studies (Turkelboom, Poesen, & Trébuil, 2008; Wijesekara et al., 2012) have presented that the land changes instigated by the intensification of urbanization, agriculture and devastated forests area cause changes in water balance in a catchment.

The arid and semi-arid regions like North Africa experience severe water shortage due to increasing population. Water scarcity is chronic and demand is projected to increase in Morocco. Agriculture alone abstracts 80% of the water and thus water scarcity greatly impacts agricultural production and rural livelihoods while climate change will intensify these impacts (Molle & Tanouti 2017). At the same time, natural water availability is affected by aridity and droughts, particularly in more humid and semi-arid areas where agriculture is predominantly rainfed. The quality and quantity of the largest percentage of fresh water represented by groundwater is under threat and is reaching stress levels. Ground water reservoirs globally are under substantial stress due to the need to meet the demands of the rapidly growing population in urban areas, and increased frequent droughts all of which have resulted in over pumping (Denizman, 2018). According to Legrouri et al., (2012) over the last 30 years, the total level of recharge in the Saïss plain has been decreasing as a result of increasing average temperature and a reduced amount of precipitation. Calder (1993) indicated that changes in land use and land cover are one of the major human induced activities impacting the groundwater system.

According to Nolan & Taber, (2007) precise estimate of regional groundwater recharge requires a good understanding of the hydrological processes in the area, which could be highly

altered by global change, land use change and human activities. When land use changes occur, hydrological processes (infiltration, evaporation, groundwater recharge) are also affected.

Remote sensing and GIS are expedient tools needed to obtain information in temporal and spatial field, which is very critical for analysis, prediction and validation of hydrological models (Venkateswarlu et al., 2014). Both Remote sensing and Geographic Information System are essential tools in obtaining accurate and timely spatial data of land use and land cover, also as analyzing the changes in a study area (Reis, 2008). Remote sensing (RS) images can effectively record land use situations and supply a superb source of knowledge , from which updated LULC information and changes are often extracted, analyzed and simulated efficiently through certain means (Singh et al., 2018). The applications of remote sening and GIS has gained popualrity globally in monitoring changes in land-use and land cover while assessing their environmental impacts (Chaikaew, 2019; Hua, 2017; Mishra et., 2016)

The impacts of land use change on water resources have been studied in the past using physically based, spatially distributed hydrological models that incorporate scenarios analysis (Ahiablame et al., 2017). The Soil and Water Assessment Tool (SWAT) is one of the mostly commonly used scenario based model, for assessing the impacts of land use on hydrological processes from watershed scales to global scales e.g (Johnson et al., 2015; Karlsson et al., 2016)

1.2 Problem statement

Morocco, has suffered from recurring droughts mainly since the 1960s, and this has greatly impacted on the precipitation and availability of water resources thus impacting the sectors like agriculture, industry and urban settlement (Bouabid & Elalaoui, 2010). Worldwide, aquifers are under severe threat of depletion and deprivation (Legrouri *et al*., 2012). The Saïss aquifer in Morocco threatens to deplete, as it is affected by declining levels of precipitation, coupled with an increase in average temperatures by 1^{o}C (Legrouri *et al.*, 2012). The resilience of the Saïss aquifer is threatened by declining and unpredictable rainfall due to climate change, and a 1^{o}C increase in average temperature (Legrouri *et al.*, 2012). According the Legrouri et al., (2012), the spring sources supplying the shallow aquifer have greatly declined since 1970 by 45%, from 24 m^3/s to 15 m^3/s. The contribution of land-use changes to the water balance in the basin is anonymous. The current condition of Saïss aquifer in regards to contribution of land use changes to the water balance of the basin is not known. The changes in land-use are however visible, as the urbanization rate of Fez city is at 49%, just slightly below the national average of 55% (Mukaya, 2017). The agriculture industry is also growing exclusively while

farmers are increasing and expanding their production, opting for high value commercial crops which are water intensive (CCAA, 2009).

The Oued Fez basin, is highly prone to flooding. The ground water usually overflows during extended rainfall events at the upstream of the Oued Fez watershed (El Garouani, et al., 2017). In as much as the flooding can be linked to excessive rainfall, there are more contributing factors to this than the above mention, therefore it is important to understand the impact of land use changes on the Oued fez Basin's water balance as a contribution to providing remedies to proper exploitation of the water in the basin and flood control.

1.3 Objectives

The main objective of this study is to simulate the impacts of land-use and land cover changes in Oued Fez basin on water balance components, using Remote Sensing, GIS techniques, and SWAT modelling. This is further sub divided into the following specific objectives:

i. To assess the changes in land-use between 1988 and 2018 within Oued Fez basin using remote sensing and ArcGIS techniques.
ii. To calibrate and validate the model for the Oued fez basin.
iii. To assess the impacts of land-use change on water balance within the Oued Fez basin.
iv. To assess the performance efficiency of the model in simulating land-use changes on water balance.

1.4 Research questions

i. How has the land-use in Oued Fez basin changed in the past 30 years from 1988 to 2018?
ii. What are the requirements for calibration of SWAT model in Oued Fez basin?
iii. What are the impacts of land-use change on the water balance components in Oued Fez basin?
iv. How efficiently did the model simulate the impacts of land-use change on water balance within the basin?

1.5 Justification

The increasing uncertainty due to climate change drives a number of activities including water resource management and allocation in Morocco. In the face of climate change, the study to assess impact of land use changes on hydrology in the Oued Fez basin will allow for better mitigation and adaptation strategies to the use of available water resources in this region.

Assessment of impacts of actual and probable land-use changes on hydrology are vital in land use planning, essentially for effective water resources management (Aduah et al., 2017)

1.6 Scope of the study

This study is limited to the assessment of the land-use change for the past 30 years using remote sensing and GIS, and simulation of land-use change impacts on the water balance components in the Oued Fez basin, located in Sebou watershed. The study was limited to hydrological modelling using the Soil Water and assessment tool (SWAT model).

1.7 Thesis Outline

This work is subdivided into 4 broad chapters; Chapter one contains the Introduction explicitly discussing the research problem, objectives, questions and the scope of this study.

Chapter two gives a general literature review related to the study and its major focus is land use changes, remote sensing and GIS techniques applications and hydrological modelling.

Chapter three broadly discusses the methods that were used for data collection and analysis. Chapter four gives the overview of the results obtained from the study, with the discussions of the same.

In the end, I highlight the thesis study conclusions and propose recommendations.

CHAPTER TWO

LITERATURE REVIEW

2 Land-use / land cover changes

Land-use and land cover (LULC) are two different terms generally assessed in combination, and are both dependent on each other (Rawat & Kumar, 2015; Turner et al., 1988). The land cover is defined by the attributes of the earth's land surface and immediate subsurface, including biota, soil, topography, surface and groundwater, and human structures while land use is defined by the needs that humans exploit the land cover (Lambin et al., 2003). Land use affects land cover and in turn is affected by changes in land cover (Rawat & Kumar, 2015). Changes in land use directly influence the hydrology of the drainage basin (Bhaduri et al., 2000; Fohrer et al., 2001; Tang et al., 2005).

Land-use changes involve conversion of existing land-use to another, or transformation into another class (Wagner *et al,* 2013). These changes are mostly impacted by the human activities, and the population growth pressure, and in turn pose severe impacts on the environment and population directly or indirectly (Mukaya, 2017). Among the effects of land-use change is the environmental deprivation and loss of biodiversity (Reis, 2008). Since land-use changes pose danger to the environment, it is important to collect data on the changes in order to make informed environmental decisions in the future.

2.1 GIS and remote sensing use in monitoring land-use and land cover changes

Use of remote sensing and GIS is rapidly increasing their role in the field of hydrology and water resources development (Venkateswarlu et al., 2014). Remote sensing provides multi-spectral, multi-temporal, and multi-sensor data of the earth's surface (Choudhury, 1999). One of the utmost benefits of using remote sensing data for hydrological investigations and monitoring is its ability to get information in spatial and temporal domain, which is extremely crucial for successful analysis, prediction, and validation (Saraf, 1999). Remote sensing techniques for LULC change detection are the most prominent methods of recent. According to Lambin et al., (2003), the use of remote sensing techniques for LULC change analysis gives good accuracy, information is obtained at low costs, it's less time consuming and with GIS, results can be updated easily at any time new data is available.

With the discovery of remote sensing and Geographical Information System (GIS) techniques, land use/cover mapping is more useful and gives a detailed way to improve the selection of

areas for various land uses including agricultural, urban and/or industrial areas of a given region (Selcuk, 2013). Lately, remote sensing has gained numerous applications in updating landuse/cover maps while it is the mostly used tool for land-use/land cover mapping (Lo and Choi 2004).

Highly valuable land use/cover data for the earth's surface for the last three decades is present as Landsat-TM images (USGS, 2014). More importantly, the whole Landsat archive is freely available to the scientific public, availing useful information for classifying and monitoring changes in manmade and physical environments (Chander et al., 2009). Land cover is a primary input for most of the existing hydrological models.

2.2 Impacts of land-use changes on hydrology

Land use changes and hydrology are interrelated, as various research studies indicate the relationship between climate, land-use, and hydrology. These studies agree that streamflow generation is to some degree dependent on vegetation type. In addition, hydrological models that consider spatial-temporal watershed characteristics are fundamental tools for accurate prediction of watershed water balance (Dwarakish & Ganasri, 2015). Land-use change poses different impacts on the hydrological components.

Several studies have investigated hydrological impacts of land-use change at watershed scales (e.g. Devia et al., 2015; Wijesekara et al., 2012). Previous studies indicated adverse effects of land use change adversely on the natural hydrologic system through increased variability in streamflow, surface runoff, ET, infiltration, subsurface flow, infiltration, and precipitation interception (e.g. Fohrer et al., 2001; Schilling et al., 2008)). For example, Schilling et al. (2008) in his research found that the average annual ET decreased with increasing corn acreage in the Raccoon River watershed in Iowa. According to Abouabdillah et al., (2010), a study conducted in semi-arid watershed in Tunisia indicated adverse effects of land use on water balance using SWAT modelling recording ET of 1436.4 mm/yr which falls within the range however a low base flow was recorded. In a study conducted in South India, the effect of LULC change shows an increase in annual streamflow by 0.77% from 1990 to 2008, whereas the mean monthly streamflow increased by 9.46% (Anil & Ramesh, 2017).

2.3 Impacts of Climate Change on hydrology

Climate changes alter the hydrological cycles and general surface and groundwater flow. The alteration directly affects the water resources, forests, ecosystems, agriculture, and the environment (Chien et al., 2013; Rwigi, 2014). Precipitation and temperature level are subject to climate change impacts, their increase lead to excess runoff and high evapotranspiration

respectively. Increased runoff in turn leads to flooding. The effects of climate change on hydrology are mostly obtained through scenarios modelled using the global climate models (GCMs) to compute the future impacts. A research conducted in the semi-arid environment of Blue Mountains, indicated that climate change would exacerbate changes on the hydrological components. Increase in precipitation would increase the flooding frequency (Clifton et al., 2018), while reduced flow in summer would lead to reduced water supply. Groundwater recharge may be described by unsaturated flow through surface humid soil, weathered clay, and fractured rock (Jinno et al., 2009). Various studies are conducted to grasp the effect of land-use/land-cover (LULC) and global climate change on hydrological processes using an integrated modelling approach (Farjad et al., 2017). Various studies have investigated the effect of climate change and land-use change on groundwater recharge (Adhikari et al., 2020; Hu et al., 2005; Owuor et al., 2016; Yun et al., 2011). Coupled effects of land-use and hydrology are seen to pose greater risks and changes on the hydrology.

2.4 Basin water balance

Water balance refers to computation of the main components of a hydrologic system, which involves interactions between surface water and groundwater systems. The water balance is used to measure the availability of water in a basin. On the basin level, the major water balance components include: precipitation, surface runoff, evapotranspiration, groundwater flow, and change in storage. Each of these components is capable of being modelled individually. Various hydrological models focus on different components of the water balance, SWAT for example models the soil water (Neitsch et al., 2009), MODFLOW models the groundwater.

Water balance is described by a general hydrologic equation expressed as:

$$\boldsymbol{Change\ in\ Storage}\ (\boldsymbol{S}) = \boldsymbol{Inputs}(\boldsymbol{I}) - \boldsymbol{Outputs} \qquad (2.1)$$

2.5 Hydrological modelling

Over the past decades, the effects of land cover/land use changes on hydrology have been evaluated using (i) field-based data-driven statistical methods, based on single catchments or paired catchments (Brown et al., 2005) and (ii) hydrological modelling (Chu et al., 2010; Warburton et al., 2010). According to Li & Coe, (2007), hydrological models using physically based tools are reported to provide a good representation of observed hydrological processes for large areas, and also enable rapid evaluation of catchment development scenarios, using comparatively less time and resources than field studies. Several water balance models have been developed in response to the given problems e.g., SWAT (Soil & Water Assessment Tool)

model (Arnold et al. 2000), WetSpass water balance model (Batelaan & De Smedt, 2001 and 2007), HBV (Hydrologiska Byrans Vattenavdelning) model.

2.6 Types of models

Classification of rainfall-run off models is based on the input parameters, and the extent of the applied physical principles of the model. Hydrological models can be classified as lumped and distributed, in relation to model parameters. Or deterministic and stochastic in relation to other criteria.

Furthermore, models can also be classified according to time factor as static and dynamic. While model classifications are vast, the most important is empirical model, conceptual models and physically based models. Other models are also classified as distributed or lumped.

2.6.1 Empirical models

These largely depend on observations, as they only account for the information from existing data without considering the hydrological processes and hence are also called data driven models. It involves mathematical equations derived from concurrent input and output time series and not from the physical processes of the catchment (Devia et al., 2015). These models are valid only within the boundaries. Unit hydrograph is a typical example of empirical models. Statistically based methods use regression and correlation models and are used to find the functional relationship between inputs and outputs. Artificial neural network and fuzzy regression are some of the machine learning techniques used in hydro informatics methods.

2.6.2 Conceptual models

They describe all the components of a hydrological process. The model therefore consists of a number of interconnected reservoirs which represents the physical elements in a catchment in which they are recharged by rainfall, infiltration and percolation and are emptied by evaporation, runoff, drainage etc. The model is supported by semi empirical equations and assessment of model parameters is not only from field data but also through calibration. A sizable amount of meteorological and hydrological records is required for calibration. The calibration involves comparison of simulated and observed values (curve fitting) which makes the interpretation difficult and hence a less degree of confidence in predicting the effect of land use changes (Devia et al., 2015). Over the years, many conceptual models have been developed with varying degrees of complexity. Stanford Watershed Model IV (SWM) is the first major conceptual model developed by Crawford and Linsley in 1966 with 16 to 20 parameters. Conceptual models are also classified as lumped or semi distributed models.

2.6.3 Physically based models

This is a mathematically idealized representation of the important phenomenon. These also are called mechanistic models that include the principles of physical processes. It uses state variables which are measurable and are functions of both time and space. The hydrological processes of water movement are represented by finite difference equations. It doesn't require extensive hydrological and meteorological data for its calibration but the evaluation of huge number of parameters describing the physical characteristics of the catchment are required (Abbott et al. 1986 a). Under this method huge amount of knowledge like soil moisture content, initial water depth, topography, topology, dimensions of river network etc. are required. Physical model can overcome many defects of the opposite two models due to the utilization of parameters having physical interpretation. It can provide great deal of data even outside the boundary and may be applied for a good range of situations. SHE/ MIKE SHE model is an example (Abbott et al., 1986 a, b)

2.6.4 Lumped models.

Lumped models treat the catchment area as a single homogenous unit. In lumped models, spatial variability of catchment parameters is overlooked (Moradkhani & Sorooshian, 2008). A lumped model is unable to simulate specific flows within a catchment as it is designed to simulate total runoff and streamflow at the only the outlet point. For this reason, lumped models adequately simulate average runoff conditions with fast computational times. Average and annual runoff conditions produced by lumped models are used for regulatory purposes that look at long-term conditions. Lumped models include a lot of assumptions about the hydrological processes and therefore normally either over-or under-estimate runoff values (UCAR, 2010). They do not consider changes within a watershed, or if the changes affect the runoff process (Uhlenbrook et al., 2004).

2.6.5 Distributed models

Fully distributed models separate the model process by small elements or grid cells. They are structured like a physically-based model therefore more relatable to the actual hydrologic process. Distributed models route the calculated runoff from each cell to the nearest cell or stream, based on physical equations used to determine flow path and natural time lags. Distributed models are data-intensive, with all input data distributed spatially and temporally. Inputs needed for a typical distributed model are Digital Elevation Models (DEM); land use imagery from satellites; gridded precipitation; soil characteristics and how they change over time; topography; and watershed characteristics such as dimensions and boundaries.

Drawbacks of distributed models are their demands for distributed data and calibrated parameters for every grid cell. If the data are not fully distributed, estimations using weighted averages are used to extrapolate data. Distributed models are also limited spatially by model resolution or by input grid size.

2.6.6 Semi distributed model

In a semi-distributed model, the algorithms are simple but physically based, thus the hydrologic system is derived from theories and principles of physics. The semi-distributed model predicts the average behaviour of a catchment based on several small homogeneous units, which are then aggregated for a few defined positions (Wilby 1997).

A semi-distributed model is capable of presenting small individual units (Wilby 1997). The model process divides the catchment into smaller areas, with different parameters for each (Rinsema, 2014). Semi-distributed models are classified by their inputs; if inputs include lumped and distributed input parameters, the model is considered semi-distributed.

Semi-distributed models consider spatial variability and land use characteristics without an overwhelming model structure (Kokkonen et al., 2001). The benefits of a semi-distributed model are fast computational time and the ability to use less data and fewer parameters than a distributed model (Pechlivanidis et al., 2011).

2.7 Description of selected hydrological models.

2.7.1 HBV model (Hydrologiska Byrans Vattenavdelning model)

The HBV model is an example of semi distributed conceptual model (Bergstrom, 1976). In this model, the catchment is divided into sub catchments, which are further divided into different elevation and vegetation zones. It runs on daily and monthly rainfall data, air temperature and evaporation. Air temperature data are used for calculating snow accumulation. The general water balance equation for HBV model is

$$\boldsymbol{P - E - Q = \frac{d}{dt}[SP + SM + UZ + LZ + Lake]} \qquad (2.2)$$

Where P is precipitation, E is evaporation, Q is runoff, SP is the snow pack, SM is the soil moisture, UZ and LZ are the upper and lower ground water zone and lakes represent the volume of lake. Different model versions are now available and are used in different countries with different climatic conditions. Degree day method is used to simulate snow accumulation and snow melt. Ground water recharge, runoff and actual evaporation are simulated as functions of actual water storage.

2.7.2 TOPMODEL

It is a semi distributed conceptual rainfall runoff model that takes the advantage of topographic information associated with runoff generation. However according to Beven and Kirby (1979), Beven et al. (1986), the TOPMODEL is considered as a physically based model as its parameters can be theoretically computed. In other words, it are often defined as a variable contributing area conceptual model. It can be used in single or multiple sub catchments using grided elevation data for the catchment area. It helps within the prediction of hydrological behaviour of basins. The major factors considered in this are the catchment topography and soil transmissivity.

The main aim is to compute storage deficit or water level depth at any location. The storage deficit value is a function of topographic index (a/tanβ) (Beven, 1986), where a, is drained area per unit contour length and tanβ is the slope of the ground surface at the location. The model uses exponential Green-Ampt method of Beven (1984) for calculating runoff and it is advised to reduce the number of parameters. The output will be in the form of area maps or simulated hydrographs.

2.7.3 Water Balance Model (WetSpass)

WetSpass also referred to as water and energy transfer between soil, plants, and atmosphere) under quasi-steady state (Batelaan & De Smedt, 2001 and 2007). The model uses both physical and hydro-meteorological parameters for simulation of the long-term average spatial patterns of surface runoff, actual evapotranspiration and groundwater recharge. The model performs better for assessing long term impacts of land-use changes on the catchment's water balance. According to (Batelaan & De Smedt, 2001). It also simulates runoff, evapotranspiration, interception, transpiration, soil evaporation and errors in water balance though the model was originally developed to compute the long-term spatially distributed recharge of a basin (Batelaan & De Smedt, 2001; Kuisi et al., 2013).

The inputs to the WetSpass model include: precipitation, groundwater depth, temperature, potential evapotranspiration, wind speed, slope, soil, and land-use maps data. (Woldeamlak & Batelaan, 2007). WetSpass in a steady-state improves the prediction of the simulated groundwater level, discharge and recharge areas **(**Rwanga**,** 2013**)**. Groundwater level is used as input to the WetSpass model in the simulation process. This allows for an obtainable stable solution for the groundwater level and discharge areas after a few iterations.

The model outputs can be analysed in different ways for example the spatial variations of recharge and runoff can be obtained as a function of land use and soil type, and then analysis

of evapotranspiration and recharge as a function of elevation (Kuisi et al., 2013). WetSpass model computes and generates time series of flow hydrographs at selected stations in a recharge areas and maps of spatial outputs. Abdollahi et al., (2019) indicated that WetSpass has been used to estimate recharge for arid regions such as Ethiopia.

2.7.4 SWAT model

The hydrologic model SWAT (Arnold et al., 1998; 1993) is physically based, semi distributed model developed to predict the impact of land management practices on water, sediment and agricultural chemical yields in large complex watersheds with varying soil types, land use and management conditions over long periods of time. It operates on a daily time step and is meant to review long-term impacts (Neitsch et al., 1999). The model was modified for the use in low mountain range regions where steep slopes and shallow soils over hard rock aquifers predominate (Eckhardt et al., 2000).

In SWAT, the basin is divided into subbasins through a topography-based delineation, each subbasin containing a tributary of the river. Each subbasin is further divided into Hydrologic Response Units (HRUs), which are unique combinations of land use, soil type, and surface slope. When simulating hydrological dynamics, the areas of the HRUs are lumped within each subbasin, which makes SWAT computationally very efficient, but this comes at the expense of losing the spatial discretization of HRUs within a subbasin. SWAT has been utilized to simulate and quantify the groundwater resources (Ali *et al*., 2012; Cheema *et al*., 2014) or the effects of drinking water or irrigation pumping on streamflow (Güngör and Göncü, 2013; Lee *et al*., 2006). However, the SWAT model has traditionally emphasized surface processes because the model only includes a comparatively simple representation of groundwater dynamics, and its output does not give any spatially explicit information on the groundwater table. In the most recent version of SWAT (v. 670), groundwater is represented by a lumped module in individual subbasins divided into a shallow and a deep aquifer. Both the shallow and the deep aquifer may contribute to streamflow as baseflow through a linear reservoir approximation, ignoring distributed parameters such as hydraulic conductivity and storage coefficients (Kim et al., 2008).

The SWAT model has been used in similar semi-arid zones such as Tunisia (Abouabdillah et al. 2014), in Morocco (Fadil et al., 2011), in Southern Italy (De Girolamo et al. 2015), in Ethiopia (Setegn et al. 2014), in Niger (Chaibou et al. 2016), and in Inner Mongolia, China (Schneider et al. 2007) and proven efficient.

2.7.4.1 Hydrologic processes in SWAT

The hydrology is divided into four segments namely; surface runoff, evapotranspiration, soil water and ground water. All equations pertaining to the processes are described in SWAT2005.

The hydrological equation used in SWAT is as below according to (Neitsch *et al*., 2005)

$$SW_t = SW_0 + \sum_{n=1}^{t}\left(R_d - Q_{surf} - E_a - W_{seep} - Q_g\right) \quad (2.3)$$

Where:

$SW_t = soil\ water\ content\ (mm)$

$SW_0 = water\ available\ to\ plants\ (mm)$

$R_d = daily\ precipitation (mm)$

$Q_{surf} =$ **surface runoff** (**mm**)

$E_a =$ **evapotranspiration** (**mm**)

$W_{seep} =$ **percolation** (**mm**)

$Q_g =$ **groundwater/low flow**(**mm**)**and t is the time in days**.

Surface runoff

Surface runoff is excess precipitation that overflows on the land. Surface runoff is the part of rainfall not infiltrated into the soil, has not been intercepted and not in depressions. Therefore, surface runoff is a contributor to streamflow in a basin. In hydrology, the three major contributors to stream flow are (i) surface runoff, (ii) interflow and (iii) groundwater flow.

Surface runoff there occurs when the rate of water application to the soil surface exceeds the infiltration rate. SWAT model provides two different surface runoff estimation methods. The SCS curve number procedures (SCS, 1972) and the Green and Ampt infiltration method (Green and Ampt, 1911).

Firstly, the SCS Curve Number method relates a calculated Runoff Curve Number (CN) to runoff, accounting for initial abstraction losses and infiltration rates of soils. The initial abstraction comprises storage on surface, interception and infiltration prior to runoff and the retention parameter. The SCS CN varies spatially due to changes in soils, land use, management and slope and due to temporal changes in soil water content. SCS curve number

is a function of soil permeability, land use and antecedent soil water conditions. The method defines three antecedent soil moisture conditions; (i) dry (wilting point), (ii) average moisture, and (iii) wet (field capacity).

The SCS CN equation is given is (SCS, 1972):

$$\boldsymbol{Q} = \frac{(\boldsymbol{R}-\mathbf{0.2}\boldsymbol{S})^{\mathbf{2}}}{(\boldsymbol{R}+\mathbf{0.8}\boldsymbol{S})} \quad (2.4)$$

where: $\boldsymbol{Q}$ = accumulated runoff, $\boldsymbol{R}$ = precipitation on that day, $\boldsymbol{S}$ = watershed retention. S is related to the soil and cover conditions of the watershed through the CN. CN ranges from 0 to 100.

Secondly, the Green and Ampt Infiltration method, was developed to predict infiltration assuming excess water at the surface at all times (Green and Ampt, 1911). The equation assumes a homogenous soil profile and uniformly distributed antecedent moisture. Mein and Larson (1973) developed a methodology for determining ponding time with infiltration using the Green and Ampt equation.

The Green-Ampt Mein-Larson infiltration rate is defined as:

$$\boldsymbol{f_{inf,t}} = \boldsymbol{K_e}\left(\mathbf{1} + \frac{\boldsymbol{\varphi_{wf}}.\Delta\boldsymbol{\theta_v}}{\boldsymbol{F_{inf,t}}}\right) \quad (2.5)$$

Where: $\boldsymbol{f_{inf,t}}$ is the infiltration rate at time t, $\boldsymbol{K_e}$ is the effective hydraulic conductivity, $\boldsymbol{F_{inf,t}}$ is the commutative infiltration at time t, $\boldsymbol{\varphi_{wf}}$ is the wetting front matric potential and $\Delta\boldsymbol{\theta_v}$ is the change in volumetric moisture content across the wetting front.

Evapotranspiration

Estimation of evapotranspiration in SWAT involves two steps; (i) the estimation of the reference evapotranspiration ET_o followed by (ii) the estimation of the actual evapotranspiration ETa.

In the SWAT documentation, three methods have been incorporated for ET_o estimation namely; the Penman-Monteith (Monteith, 1965), Priestley-Taylor (Priestley and Taylor, 1972) and the Hargreaves methods, (Hargreaves, et al., 1985). Each of the above methods is used under different conditions and vary according to the number of inputs required however Penman Monteith is the most commonly used method in SWAT.

Once ET_o is determined, SWAT computes the ETa. First, rainfall intercepted by the plant is allowed to evaporate, and the SWAT calculates the maximum amount of plant transpiration,

and maximum amount of soil evaporation (Neitsch, et al., 2005). If the Penman-Monteith method is selected for computation of evapotranspiration, potential daily transpiration is calculated using the extended application of Penman-Monteith equation that directly calculate any crop evapotranspiration using the surface and aerodynamic resistance of the specific crop (Neitsch et al., 2005).

Soil water

Water movement in the soil undergoes various processes, they include: infiltration, evaporation and or plant uptake, lateral flow and percolation to the bottom layers.

SWAT only simulates saturated flow directly, while the unsaturated flow between soil layers is indirectly modelled with the depth distribution of plant water uptake. The soil layer is divided into multiple layers. Once the field capacity of a soil layer is exceeded, saturated flow takes place. The excess water is then available for percolation, lateral flow or drainage (Neitsch, et al., 2005).

Groundwater

Groundwater contribution to streamflow is simulated by creating shallow aquifer storage (Arnold, et al., 1993). Percolation from the bottommost layer of the soil profile recharges the shallow aquifer (groundwater recharge). The shallow aquifer also contributes base flow to the main channel in the basin (Neitsch, et al., 2005). Total groundwater recharge is simulated by SWAT as: water that passes past the bottom of the soil profile, channel transmission losses, and seepage from the ponds or reservoir. Water that moves past the shallow aquifer to the deep aquifer is assumed to be contributing to streamflow somewhere out of the watershed bounds.

Water balance equation for shallow aquifer is:

$$\boldsymbol{D_{s,i} = D_{s,i-1} + R_s - Q_g - revap - P_s} \qquad (2.6)$$

where; $\boldsymbol{D_{s,i}}$ is the shallow aquifer storage on day i, $\boldsymbol{D_{s,i-1}}$ is the shallow aquifer storage on day i-1, $\boldsymbol{R_s}$ is the recharge entering the shallow aquifer, $\boldsymbol{Q_g}$ is the base flow/ ground water flow into the main channel, $\boldsymbol{revap}$ is the water taken up by soil in response to water deficiencies on that day, $\boldsymbol{P_s}$ is the water withdrawn from shallow aquifer by pumping.

CHAPTER THREE

METHODOLOGY

This chapter describes the methods used to model the impacts of land use changes in the Oued Fez basin, which is part of the Saïss plain. The tools used to conduct the study involve remote sensing techniques, GIS and SWAT model. Hydrological modelling was used to model impacts of LULC on water balance.

3 Description of study area

Oued Fez is an urban catchment with >10% of its area is occupied by the city of Fez. The Oued Fez basin, which is part of the Saïss plain covers an area of 879 km²; it is located in the central-eastern part of Morocco and lies between latitudes 33°30' and 34°08'N and between longitudes 4°54' and 5°09'W. The basin is characterised by three different topographic units Hydro-climatologic context. The basin is drained by the Oued Fez; an intermittent river and also the main river in the basin. The river is a tributary of the Sebou river, the biggest river system in Morocco.

3.1.1 Topography of the watershed

The Middle Atlas plateaus in the south, which have the highest area and elevation, located between the Rif range to the north and High Atlas range to the south. They are stepped plateaus from the South (Immouzzer Causse: 2020 m) to the North (Sefrou Causse: 1400 m). This morpho structural unit is mainly formed by massive limestone formations and Liasic dolomites which rest in discordance on Triassic clays.

The lowest part of the watershed corresponds to the Saïss plateau (400 to 700 m), with a gentle slope from South to North. It is a depression between the limestones and dolomites of the Lias and the complex Dogger formations.

The northern part of the catchment area is limited by the prerifaine Rides which appear as a medium-high mountain (Jbels Tghat, 860 m and Zalagh, 900 m). This mountain is mainly characterised by limestone formations.

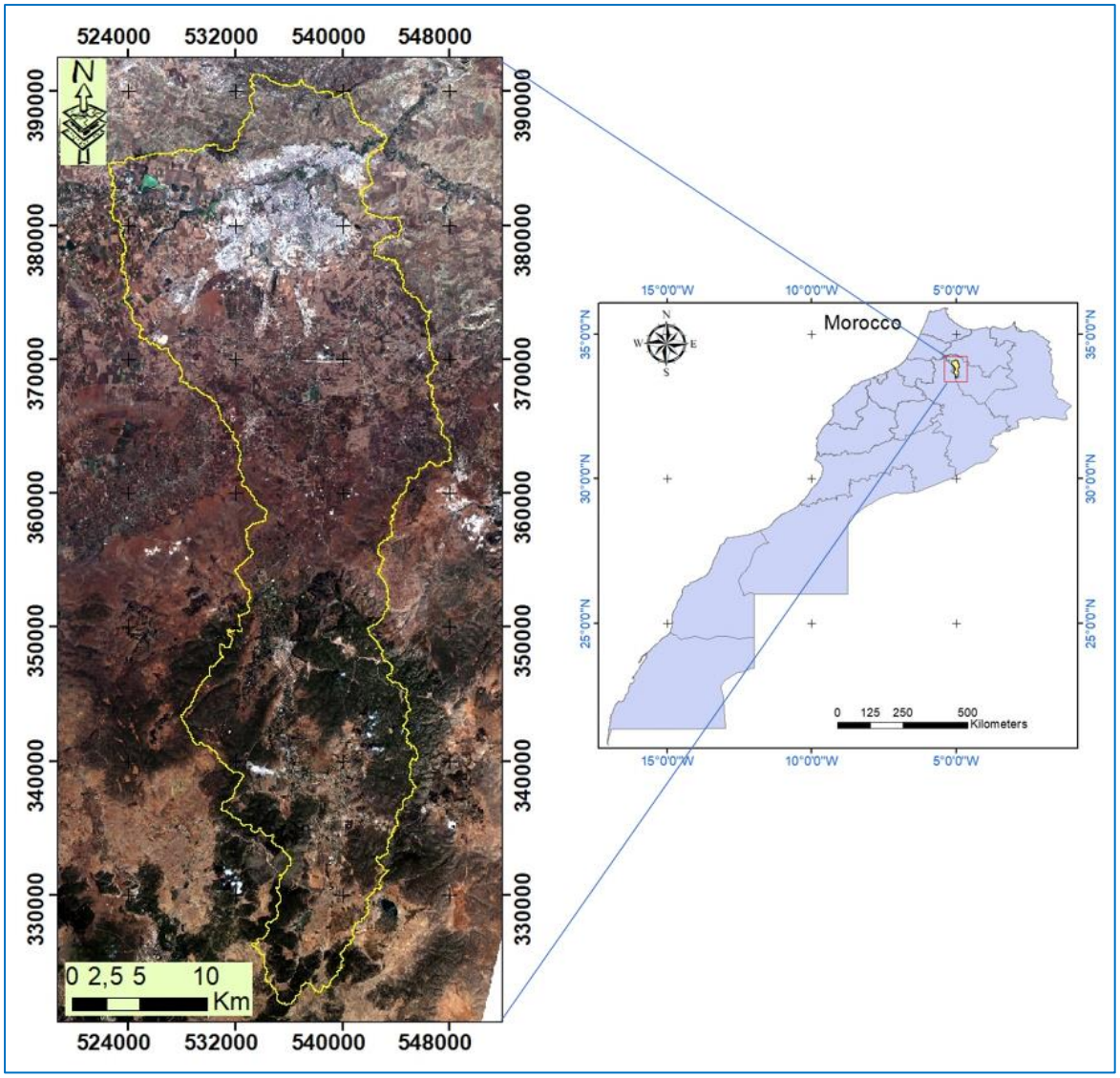

Figure 3.1: Location of Oued Fez basin.

3.1.2 Population

The Oued Fez basin has Fez as the major city with a population of over one million inhabitants. Throughout its history, Fez has undergone major changes, and today it is an urban area covering an area of about 100 km². The population growth rate in the area is approximately 3 to 5 % per year (HCP, 2015). The table below shows the population in the region

Table 3.1: Population of rural and urban households in Morocco, projecting Fez city (HCP, 2015)

Population	Urban	Rural	Total
Fez city	1,129,768	20,363	1,150,131
Fez-Meknes region	2,564,220	1,672,672	4,236,892
National level	20, 432,439	13,415,803	33,848,242

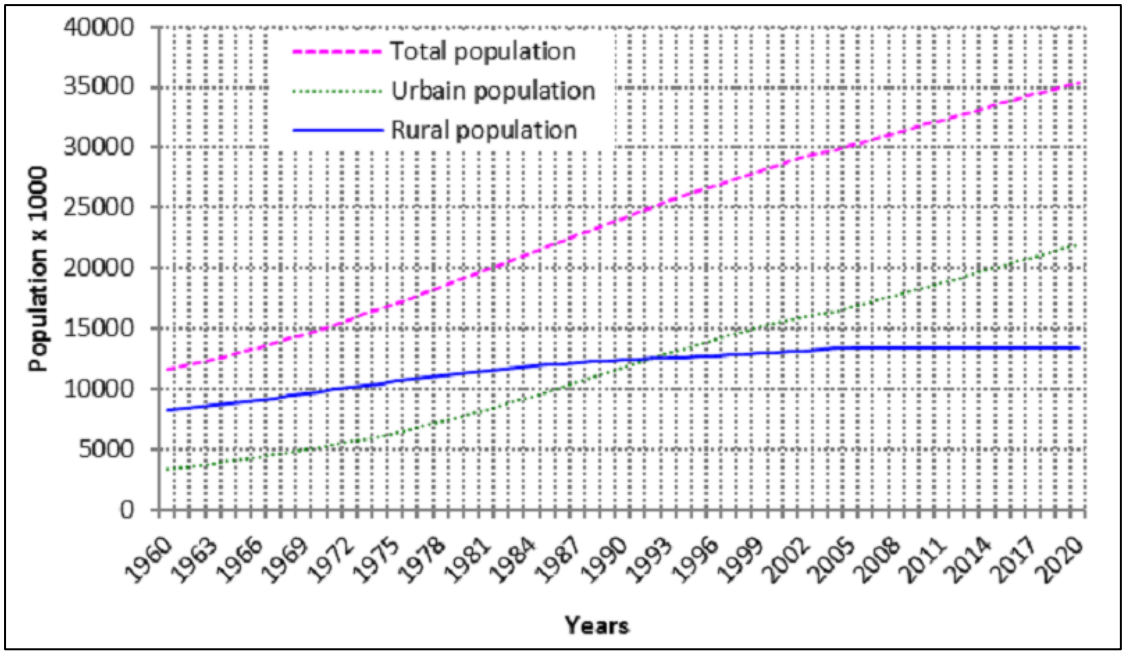

Figure 3.2: Rural and urban population growth in Morocco

Source: (El Garouani et al., 2017; HCP, 2015)

3.1.3 Climatic conditions

The watershed is characterised by a Mediterranean climate influenced by the continentalism. It is marked by a pronounced contrast between a hot and dry summer and a cool and humid winter, as well as by an irregular rainfall, the latter decreasing from South to North.

3.1.3.1 Rainfall

Precipitation data recorded at Sebou Hydraulic Basin Agency (ABHS) station shows a high inter and intra-annual variation of rainfall, a feature typical of semi-arid climates.

The average annual rainfall across the basin is between 400 and 550 mm. For the Fez region, average monthly precipitation varies between 2 to 70mm as shown in graph below, with the highest values recorded in November.

The annual rainfall distribution is characterised by heavy rainfall in autumn, a slight decrease in winter with a relative maximum in early spring and a very dry summer. The period of October to May has the heaviest amount of rainfall recorded, with 9 to 10 rainy days per month for an annual average of 84 rainy days.

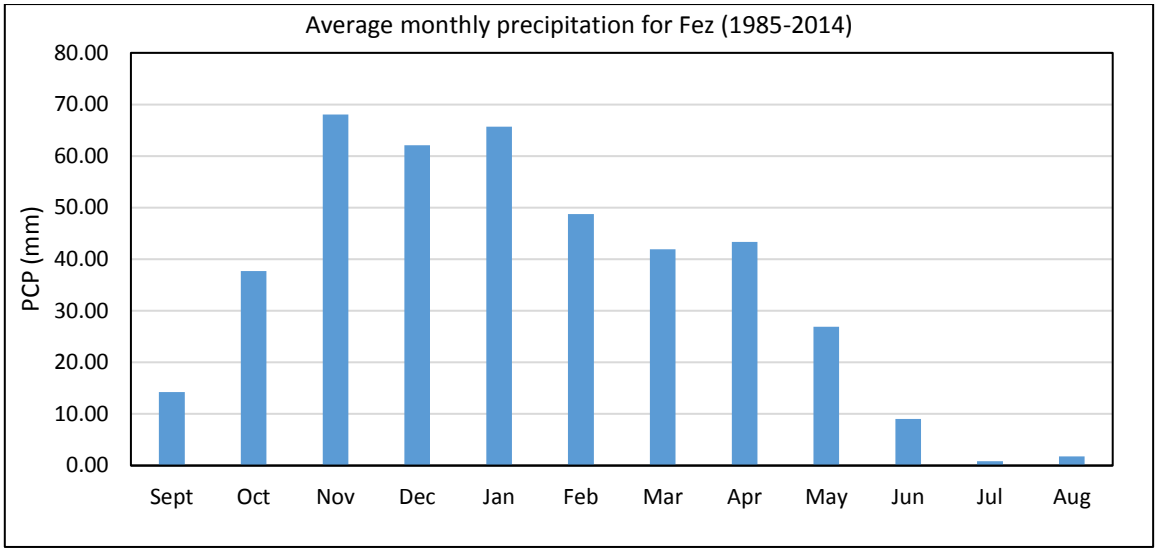

Figure 3.3: Average monthly precipitation of Fez region at Fez-Saiss Station.

3.1.3.2 Temperature

The region's temperatures vary, in winter it is either cold, warm or hot with minimal temperatures especially in Fez where low temperatures transition into frosts. In summer, temperatures range between high to moderate with maximum temperatures during the day and low temperatures in the night. Maximum temperatures are recorded in July and August with average of 37°C. The temperatures generally range between 10 and 25℃. The average annual maximum temperature is 37 °C, while the minimum temperature is 6 °C. Average monthly maximum and minimum temperatures for the period (2000-2015) are shown in the graph below The mean monthly temperature recorded at the ABHS station over the 1978- 2008 period is 16.8°C and is similar to the values calculated at Fez airport for 1961- 2003 (ABHS, 2004).

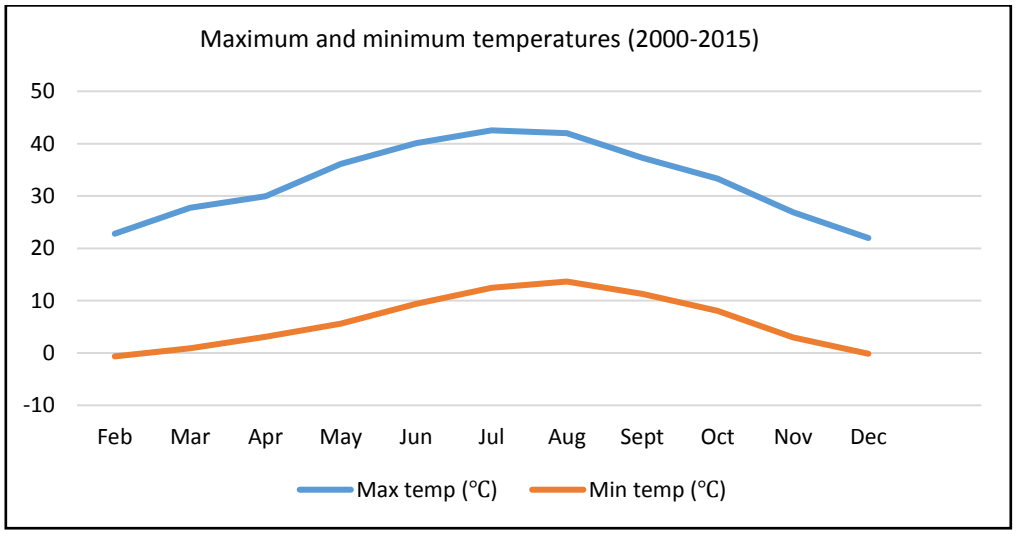

Figure 3.4: Average maximum and minimum monthly temperatures of Fez region at Fez-Saiss Station.

3.1.3.3 Evapotranspiration

High variations are also observed for the potential evapotranspiration data. PET can reach 163 mm during July and drop to 25 mm in January (ABHS, 2004). It reaches a maximum in July-august with ca. 160mm/month and a minimum in December-January with less than 50mm/month. The average monthly potential evapotranspiration for the region over the period (1985-2014) is shown in the graph below. The highest ET values are recorded in July, while the lowest are recorded in Jan. The high PET combined with low or null precipitation yields water stress throughout the summer months.

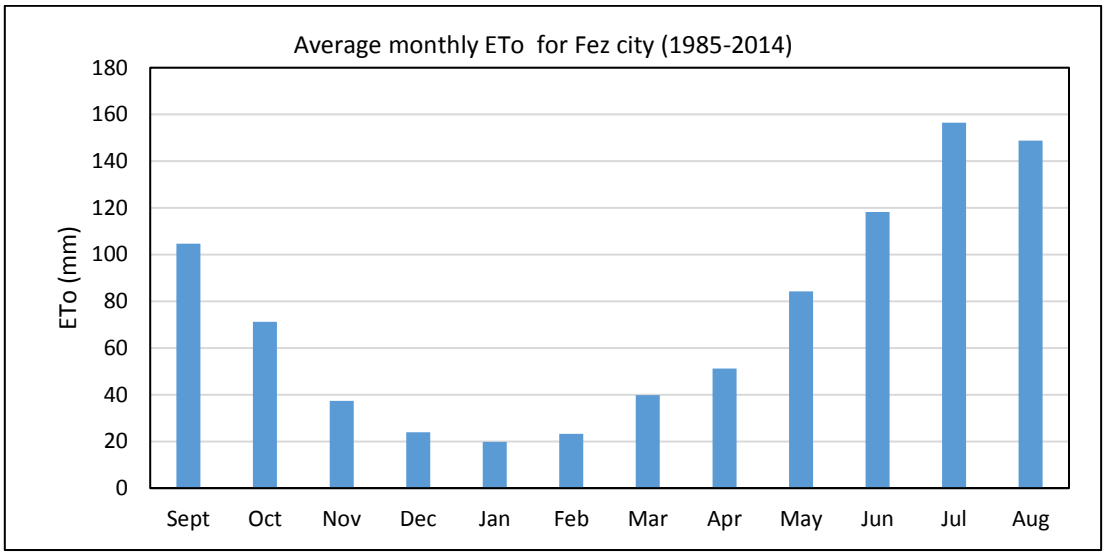

Figure 3.5: Average monthly potential evapotranspiration of Fez region at Fez Saiss Station.

3.1.4 Hydrology

The Oued Fez catchment area (879 km², average slope of the main Oued = 2.18%) drains a relatively dense hydrographic network (Dd = 1.68 km/km²); it is composed of several sub-basins of different sizes and morphologies, namely: Oued Boufekrane (52.40 km², average slope = 2. 87%); Oued El Mehraz (52.40 km², average slope of = 2.81%); Oued El Himmer (80.74 km², average slope = 3.68%); Oued Chkou (428.08 km², average slope = 4.68%); Oued Chkou (428.08 km², average slope = 3.68%); Oued Chkou (428.08 km², average slope = 3.68%); Oued Chkou (428.08 km², average slope = 3.68%); Oued Chkou (428.08 km², average slope = 3.68%); Oued Chkou (428.08 km², average slope = 3.68%); Oued Chkou (428.08 km², average slope = 2.43%) and Oued El Malleh downstream of the catchment area (34.03 km², average slope = 2.8%) as well as other less important tributaries.

The Fez (main river), which flows from west to east from its sources of Ras El Ma to Sebou crossing the old medina of Fez, the Oued Fez receives several tributaries throughout its path towards the Sebou river, and its sources of water include: resurgences of groundwater as the

Oued Mahraz, Oued Miyet and Boufekrane, and others that drain essentially runoff water: Oued Mellah, Oued Smen, and Oued Ain chkef.

The agglomeration of Fez is located in the confluence zone of the basin's hydrographic network. Since its creation, twelve centuries ago, its first core (the medina of Fez) has found in its location near the Oued Fez and some springs a strategic location to meet its various water needs.

3.1.4.1 Ground water

The region harbours part of the Saïss aquifer system, is comprised of two superimposed and connected aquifers, an unconfined shallow phreatic aquifer (Saïss aquifer) and a deep Liassic confined aquifer. These aquifers are the major supply of drinking water and irrigation water demand and therefore play an important role in the socio-economic development of Fez-Meknes region. The unconfined Saïss aquifer is mostly used by the private sector. Both aquifers are over-exploited and falling piezometric levels have been reported for both (ABHS, 2006).

An unconfined aquifer circulating in the sands, sandstones, conglomerates and Sahelian Pliocene lacustrine limestones and locally in the travertine. Tortonian deposits of marl are the nature impermeable bedrock of the aquifer. Their thickness can reach 900 m and put in charge the deep aquifer. The average depth of the water table from the ground surface level is 25 m.

A confined aquifer circulating in dolomitic limestones of the Lias and will start charging under the thick series of impermeable marl Miocene. The depth from the base of the Liassic formations varies between 0 m in the south of the basin and over 1000 m at its northern limit in contact with the prerif formations.

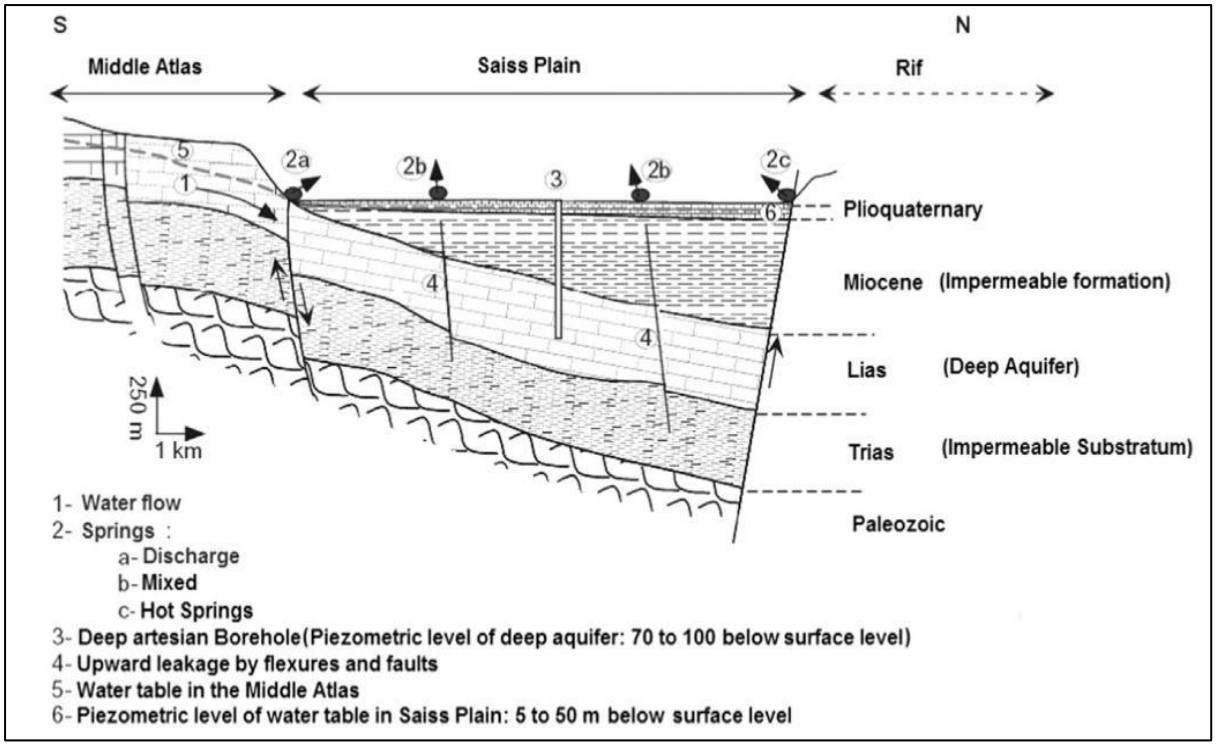

Figure 3.6: Showing the aquifers in Saïss plain.

(Belhassan, 2010; Laraichi et al., 2016).

3.1.5 Aquifer recharge

The water supply for human activities in the watershed comes from three locations: a shallow aquifer located in the Plio-Pleistocene sediments, a deep aquifer located within the Liassic dolomites and limestone, and various springs located in the region. The recharge of aquifer located inside the Saïss basin is largely controlled by precipitation occurring in the Middle Atlas (Amraoui, 2005; Belhassan, 2011). The annual variation of precipitations influences the refill of aquifers in the basin. The Saïss aquifer has experienced increasingly unsustainable levels of exploitation since 1980.

3.1.6 Geology of Oued Fez watershed

The geology of Fez is characterized by the presence of lacustrine limestone, clay-limestone tuffs and conglomerates on set, silt in the alluvial terraces of the Sebou Valley, travertine, marls, and conglomerates in the valley, debris of limestone slopes, limestone, sandy loams, tuffs and conglomerates on north glaze reliefs, and blue marls altered on the southern hills.

Lithological formations remain an essential element that influence surface and underground flows. On the Saïss plateau, a mio-plio-quaternary filling depression overcomes the limestones and dolomites of the Lias and the complex Dogger formations, and the Liasic formations rest directly on the Triassic substrate with the wrinkles of the ridges of the prerif mountains

3.1.7 Economic Activities

The major economic activities in the region are agriculture, industry, craft, tourism and trade. The agricultural and industrial economy contributes greatly to the national economy.

3.1.7.1 Agriculture

The Oued Fez watershed is a fertile area of great agricultural production with major economic interests. The basin provides water for 1.8 million people, and is also home to 8000 commercial and subsistence farms, constituting a quarter of Morocco's arable land. These farms represent about 37,000 hectares of irrigated land, of which the largest proportion, 45 percent, are irrigated by pumped water, 32 percent are irrigated with surface water and about 22 percent are drip irrigated. The major crops grown in the basin include: grain crops (60%) with the biggest share of landuse, the others include fruit plants (14.4%), legume plants (6.6%), industrial crops – sugar beet and cane (4.2%), oilseed crops (3.6%), vegetable crops (3.1%) and forage (1.7%).

3.1.7.2 Industry

The industrial sector is very developed within the Sebou basin, especially within the agribusiness (oil, sugar), leather and textile i.e water consuming activities. The city of Fez comprises 62% of the industrial fabric of the Fez Meknes Region, occupies a privileged place in the national industrial fabric and participates in the socio-economic development of the Region and consequently of the Kingdom of Morocco. Main products exported include: cables for the automobile industry, ready to wear, semi-finished leather, leather goods, canned olives and capers, edible gum, olive oil etc.

Agribusiness: There are around 200 major mills, producing 120,000 tons of vegetable oil and 70,000 tons of vegetable oils, representing over 65% of national production. Approximately 184,000 tons of sugar is produced annually in the basin, which accounts for half of national production. Textile and leather industry: is highly developed in the basin, as the region has a large number of tanneries especially in Fez, Meknes and Kénitra cities, and produces 60% of national production. These tanneries however are a major cause of pollution of the Sebou river downstream. The city of Fez is home to nearly 614 industrial establishments.

3.1.7.3 Crafts

The city of Fez is considered the capital of craftsmanship. It harbours the majority of craftsmen and craft activities. It displays 16% of the national turnover. The main craft activities are: ceramics and pottery, tapestry, woodwork, basketry, basketry, gold, silver, copper and copperware, silk and embroidery, leather goods, leather clothing, wood carving and painting,

ironwork ... etc. The city of Fez had 52,888 artisans in 2015 (Regional Directorate of Crafts of Fez).

3.1.7.4 Tourism

The city of Fez has a highly developed tourism sector, mainly cultural tourism, distinguished by its internationally renowned historical and architectural heritage. It is also contains a rich natural, cultural and historical capital that can be a lever for the development of tourism. Fez, is a tourist destination with multiple cultural and natural assets: including an ancient medina (280 ha) classified as a world heritage site by UNESCO in 1981.

3.2 Land use classification for 1988 and 2018.

Cloud free Landsat 5 TM and Landsat8 OLI-TIR images of years (1988-08-29 and 2018-06-29) respectively of Oued Fez basin were used to classify the land use and cover changes of the selected years. The 30m resolution Landsat 5 ETM and Landsat 8 images in GeoTiff format were downloaded from USGS earth explorer website for the months of August and June respectively. These were then exported to ArcGIS and classified accordingly. Different methods of LULC classification broadly separated into supervised and unsupervised methods exist. For this study, the supervised classification was used and 7 land cover classes were identified namely: (i) arable lands (bare soil & cereal), (ii) forests, (iii) range lands, (iv) irrigated lands, (v) urban, (vi) arboriculture (olive trees & orchards), and (vii) water.

Supervised classification requires the user to have a prior knowledge about the existing land uses and land cover, and therefore the user bases on this to identify the classes existing in a Landsat image by assigning values. Training samples are sets of pixels that represent what is recognized as a discernible pattern, or potential class. The classification was conducted in ArcGIS with the help of the Spatial Analyst tool. Training samples were selected accordingly and all samples belonging to same class merged. A signature file is then created which aids in the creation of the supervised classification.

The maximum likely classification (MLC) was used to perform a supervised classification for the different LULC. MLC is a pixel based technique relying on a multivariate probability density function of classes (Richards & Jia, n.d.). The MLC method uses training samples which are obtained from the image to be classified. These are then computed to assign a particular pixel to a class with maximum probability.

The land use land cover maps for 1988 and 2018 were respectively prepared using the MLC supervised classification method.

3.2.1 Land use/cover change detection and analysis

After the land-use change is conducted, other methods are used to conduct a change analysis on the land-use. This includes calculation of area, and other associated physical changes noticed by visual inspection. The changes that occurred are interpreted to give the differences in images in terms of the before and after. Two classified images of 1988 and 2018 were compared and the figure 3.5 below indicates the areal percentage change between the two periods.

3.2.2 Accuracy assessment of classification

The LULC classification results are assessed to test the validity and dependability of the developed classified maps. A number of methods are used to assess the accuracy, including use of google maps, collecting ground truth data. Collection of ground truth data is sometimes difficult and expensive to collect the data. It is generally a complex process. Therefore, with new developments, one can collect ground truth data by using google earth.

(Congalton**,** 1991**)** recommended the use of a stratified random sampling scheme for accuracy evaluation. For the sample size, (Congalton, 1991) emphasized the need for a balance between what is statistically sound and what is practically attainable. Research recommends that the rule of thumb, a minimum of 50 samples for each land use/cover category to produce an error matrix (confusion matrix). Error matrix is a square array of numbers that presents summary information on units classified as map land cover class and reference class (Lewis & Brown, 2001). According to **(**Foody**,** 2002**),** three accuracies namely overall, user's and producer's accuracy all derived from the error matrix are used to describe the map accuracy**.** Overall accuracy is the percentage of correctly classified pixels in a sample size, it compares how the various pixels are correctly classified versus the ground truth conditions. User's accuracy describes the percentage of a correctly classified pixels for a particular class, it is also a measure for the errors of commission while producer's accuracy, also used to measure errors of omission shows how well a land cover class relates to the percentage of validation sites classified correctly. (Bai, Feng, Jiang, Wang, & Liu, 2015).

Alternatively, the Kappa test is also used to complement the accuracy assessment. The kappa index is more superior to the other accuracy measures because unlike the overall, producer's and user's accuracies, which make use of the principal diagonal, columns and rows of the error matrix, it makes use of all the information in the error matrix in order to take into account the chance allocation of class labels. Both the error matrix and kappa coefficient have widely been used in various studies to assess the accuracy of image classification.

In this study, an error matrix was generated to assess the accuracy of classification and the overall, producer and user's accuracies were calculated, with the errors of omission and commission. Random points were collected to do the accuracy assessment, a total of 379 and 362 points were collected for 1988 and 2018 images respectively. The number of random points per class varied due to the large difference in dominance of various land covers like arable land for which the greatest number of pixels were allocated, Google Earth was then used to collect/confirm the ground truth data. In addition, a kappa index was also computed. And table 3.2 indicates the rating for Kappa statistics.

Table 3.2: Rating of kappa statistics.

No	Kappa statistics	Strength of agreement
1	<0.00	Poor
2	0.00-0.20	Slight
3	0.21-0.40	Fair
4	0.41-0.60	Moderate
5	0.61-0.80	Substantial
6	0.81-1.00	Almost perfect

Source: (Rwanga, 2013)

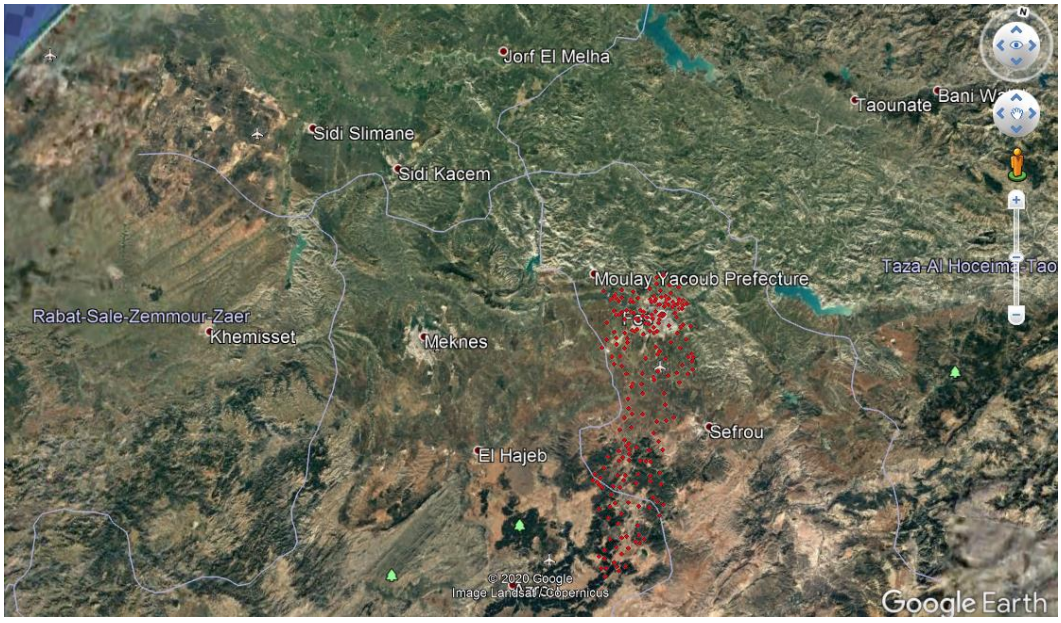

Figure 3.7: Ground truth points in google earth

3.3 Data preparation for hydrological modelling

The data used in this research was mainly collected from secondary sources. The model requires a vast number of data, including daily weather data, a DEM, Soil map and soil codes,

Land use & land cover map and LULC codes. All the data to be used in the model should be prepared according to the SWAT format which is described in the ArcSWAT 2012 documentation. The input data files are given in the table below. The SWAT version used in this study is the 2012 edition (Arnold et al., 1998).

Table 3.3: Input parameters for SWAT model.

Data	**Location**	**Period**	**Data source**
Hydro-climatic data			
Daily precipitation	(5.0081,34.0129), (-4.9993,33.6808)	1985-2018	ABHS, https://data.chc.ucsb.edu/products/CHIRPS-2.0/africa_daily/tifs/p05/
Maximum and minimum temperature	(5.0081,34.0129), (-4.9993,33.6808)	1985-2018	NASA power prediction https://power.larc.nasa.gov/data-access-viewer/
Wind speed*			
Relative humidity*			
Solar radiation*			
Streamflow	Oued Fez	Calibration(2009-2011)	(Perrin et al., 2014)
Other data			
Digital Elevation Model (DEM)	Oued Fez	N/A	NASA- *EARTHDATA*
Soil map	Oued Fez		FAO-UNESCO global soil map http: //www.fao.org/nr/land/soils/digital-soil-map-of-the-world/en/
SWAT Soil parameters	Oued Fez	N/A	http://www.indiaremotesensing.com/p/s.html
Landsat images	Oued Fez	1988, 2011 & 2018	USGS earth explorer
* Needed for computation of Potential Evapotranspiration in SWAT			

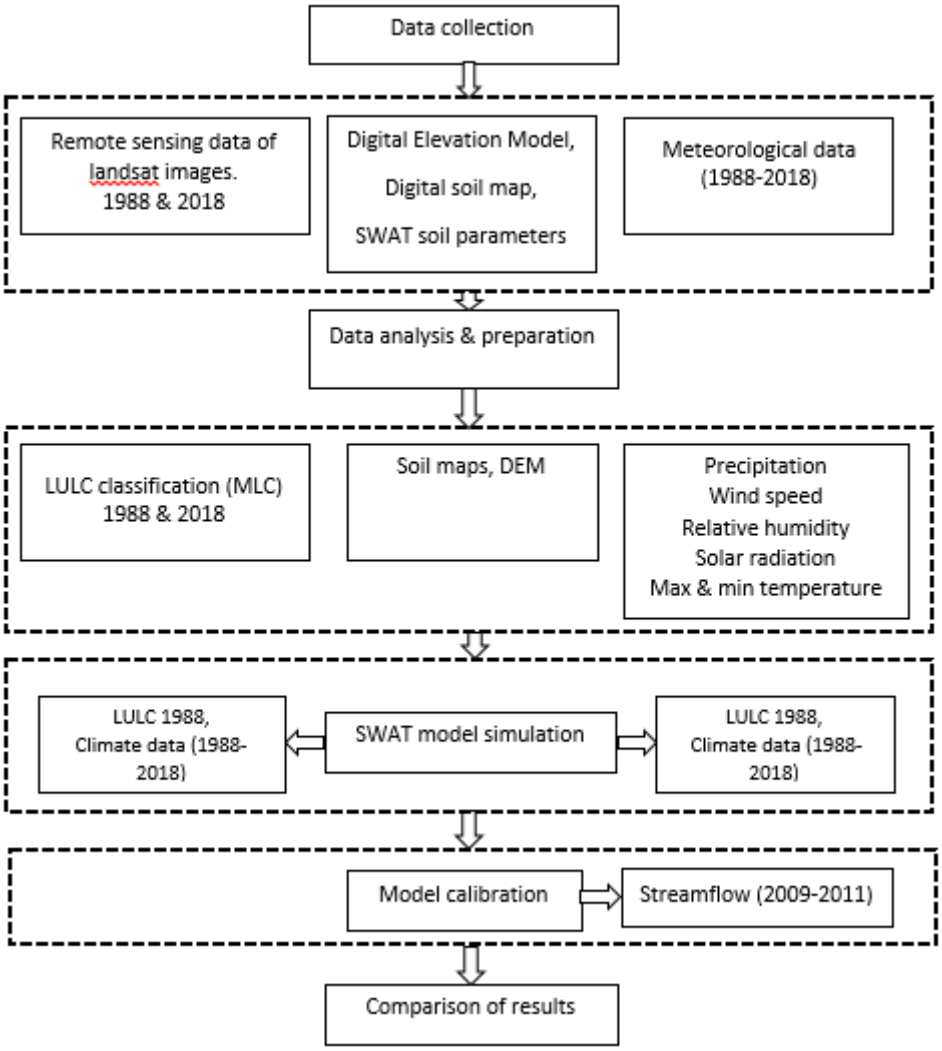

Figure 3.8: Graphical representation of methodology.

3.3.1 Digital Elevation Model (DEM)

The digital elevation model for the study area covering Fez was obtained from *NASA-EARTHDATA* website, with a cell size of 12.5 m. The DEM is downloaded in GeoTiff format and then exported to ArcGIS. A slope map is automatically derived from the DEM.

3.3.2 Weather data

The SWAT model requires weather data on a daily or sub-daily time step. Daily weather data for precipitation, minimum and maximum temperature, solar radiation, temperature and relative humidity are required to run the model. Two stations were used with coordinates (34° 0' 46.44"N, 5° 0' 29.16"W) and (33° 40' 50.88"N, 4° 59' 57.48"W) to represent the upper and lower parts of the basin respectively.

Weather data from 01/01/1985 to 31/12/2018 was downloaded from the Nasa Prediction of Worldwide energy resources website (https://power.larc.nasa.gov/data-access-viewer/), for

Solar radiation, maximum and minimum temperatures, relative humidity and wind speed all at 2m, while the daily rainfall was obtained from the CHIRPS rainfall data (https://data.chc.ucsb.edu/products/CHIRPS-2.0/africa_daily/tifs/p05/). In addition to the above data, some data was obtained from the Sebou Hydraulic Basin Agency (ABHS).

The data was checked for any missing data, or outliers before being used in the model. All missing values are indicated by a value (-99), however the data downloaded was complete with no missing data values. The climatic data was thereafter prepared according to the required format. The weather generator tool in SWAT assists in filing in missing weather data.

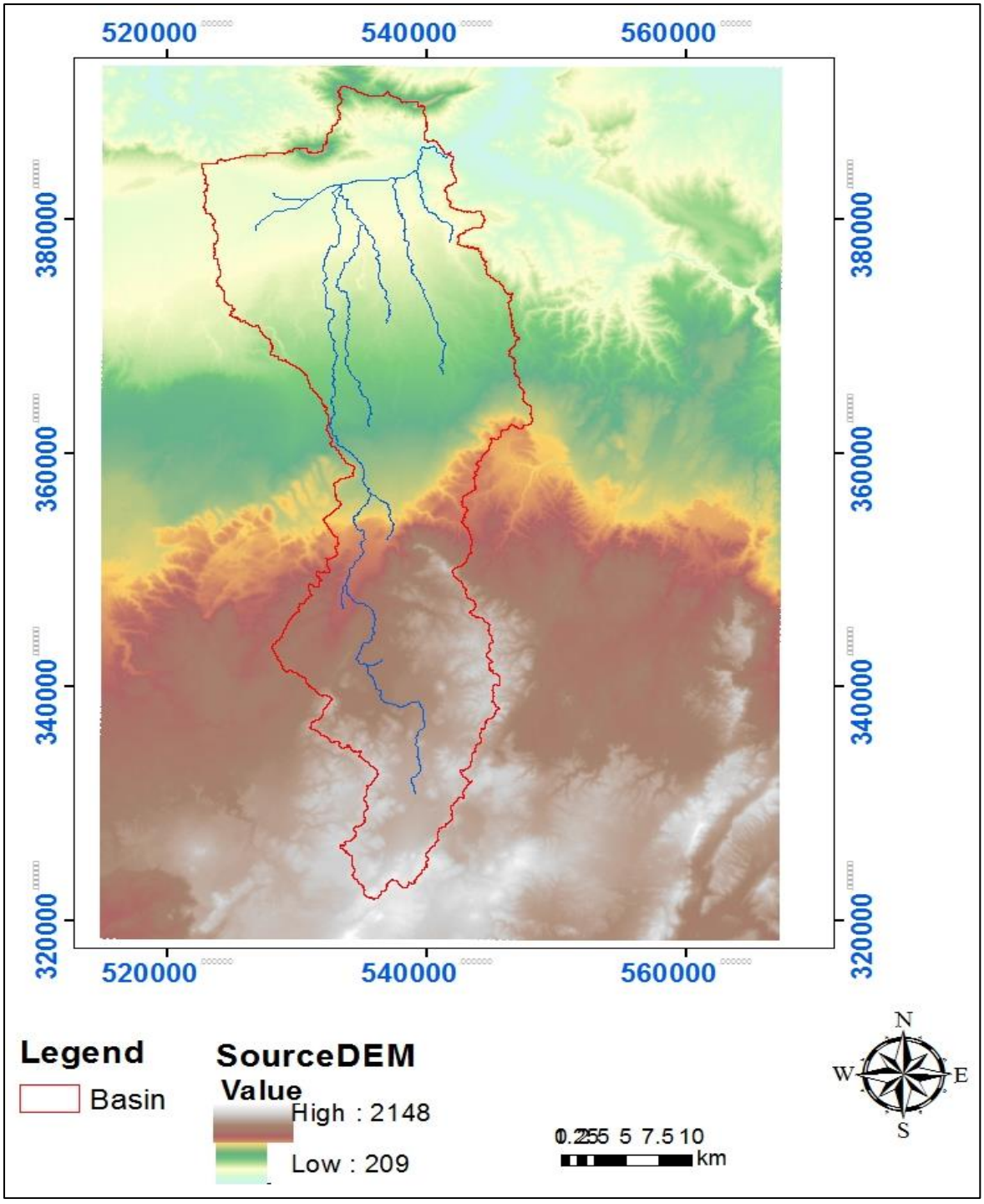

Figure 3.9: Digital Elevation model.

3.3.3 Soil data

The soil map was obtained from the FAO GeoNetwork website, as "FAO Unesco digital map of the world" in ESRI format at a scale of 1:5000000. It was exported to ArcGIS and processed accordingly to suit the study area. The study area is extracted from the World soil map by adding the Morocco shape file which is thereafter converted to raster. A User soil text file, FAO soil was used to describe the soil names and type. The corresponding soil properties were

downloaded from www.indiaremotesensing .com. All the soils in the study area belong to the hydrologic soil group D, with the dominating soil texture being clay loam. The soil map is represented in figure 3.11

Table 3.4: FAO User soil

FAO soil code	Soil name	Soil Texture	HYDGRP	Area (%)
Kk 10-3a-1391	Calcic Kastonozerns	Clay Loam	D	42.26
Kk 11-3b-1392	Calcic Kastonozerns	Clay	D	12.46
Kk 14-2b-1395	Calcic Kastonozerns	Loam	D	2.39
Lc 45-3bc-1411	Chromic Luvisols.	Clay loam	D	42.88

The soils classified for the study area are a characteristic of semi-arid and tropical Mediterranean climate and belong to two broad categories of soils namely: the Chromic luvisols, characterized by carboniferous: metamorphic rocks, Jurasic: limestone and dolomite, while the Calcic Kastonozerns are composed of alluvial deposits, limestone, sandstone, schist and sandy marl, they are also suitable for olives, figs and vines farming.

3.3.4 Land use and land cover

The LULC map was prepared in ArcGIS using the Landsat8 OLI-TIRS and Landsat5 TM images with 30m resolution. They were obtained from the USGS earth explorer website, for the dates (1988-08-29 and 2018-06-29) respectively. A supervised classification was carried out for both images by taking training samples and assigning a signature file after the classification is done. For the LULC map to be used in Swat, a land use code is required defined by SWAT and the codes used are shown in table below.

Table 3.5: Showing the SWAT land use codes.

LULC	SWAT name	SWAT code
Water	Water	WATR
Irrigated agriculture	Potato	POTA
Forest	Forest-mixed	FRST
Arable land	Agricultural land generic	AGRL
Range land	Pasture	PAST
Arboriculture	Orchard	ORCD
Urban	Residential medium density	URMD

3.4 Streamflow data

The Oued Fez data was adapted from the collected data between the period 2009 and 2011. This was the only data used during the calibration period. Shown in table (3.6), is the 17 random points available for flow data collected between 2009 and 2011. There was no data available for validation and therefore an assumption that if the calibration was satisfactory then the validation result were satisfactory.

Table 3.6: Stream flow data for the period 2009-2011.

Date	Discharge (m^3/s)	Hydrological conditions
09-Jun-09	1.7	Low flow
20-Oct-09	2.6	Low flow
11-Nov-09	2.1	Low flow
15-Dec-09	2.7	Low flow
03-Feb-10	3.3	High flow
24-Mar-10	7.9	High flow
21-Apr-10	5.3	High flow
18-May-10	4.6	High flow
23-Jun-10	1.6	Low flow
12-Jul-10	2.8	Low flow
01-Sep-10	1.2	Low flow
15-Dec-10	6	High flow
09-Feb-11	5.6	High flow
29-Mar-11	5.6	High flow
14-Jun-11	3.4	High flow
13-Sep-11	2.3	Low flow
06-Dec-11	3.4	High flow

Source: (Perrin et al, 2014)

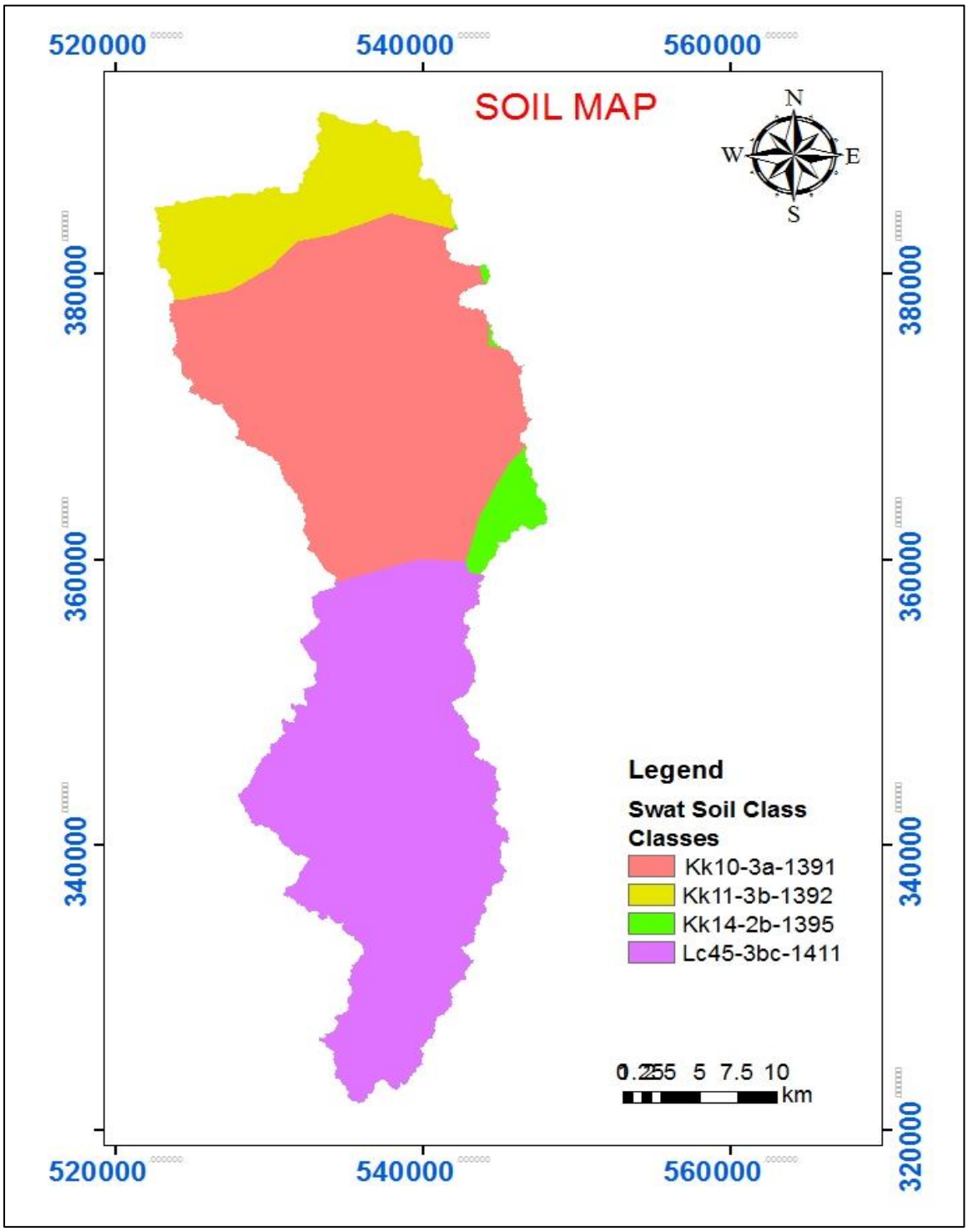

Figure 3.10: Soil map for the watershed

3.5 Determination of water balance components under different land use

The effects of land use change on water balance components were examined using the Soil Water and Assessment Tool (SWAT) (Arnold et al., 1998; Arnold & Fohrer, 2005). The SWAT model operates in link with the Geographical Information System (GIS). The SWAT calculates

the water balance in Hydrological Response Units (HRUs), which require basic information on topography, land use, soil types and climatic data (Fontes Júnior & Montenegro, 2019).

3.5.1 Watershed delineation and HRU analysis

The model operates on the principle of automatic delineation, which is carried out on the DEM.

A minimum drainage area of 3000 ha was used for DEM processing and stream flow network derivation, additionally the basin was divided into 17 sub basins. The Oued Fez was used as the main stream in the delineation. Outlet and subbasin selection were done manually by adding the catchment outlet at a known point on Oued Fez and the delineation process was completed by calculating sub-basin parameters.

The HRU analysis preceded the watershed delineation and the Hydrologic response Units are defined by the land use/land cover, soil map and slope. HRUs are lands with similar characteristics i.e. topography, land use/land cover and soil types. The water balance components are therefore determined on an HRU basis, with the assumption that similar HRUs would have similar hydrologic characteristics (Neitsch et al., 2009; Winchell et al., 2013; Neitsch et al., 2011; Arnold et al., 2012;). The analysis involves two major steps, (i) land use, soils, and slope definition, (ii) hydrologic response unit definition.

A land use map was added and land use classes were defined according to the SWAT documentation (Winchell et al., 2013). Similarly, a soil map which was earlier prepared from the FAO digital world soil map was loaded into the model and soils defined according to the FAO soil text file. The slope was also defined by the modeller and 3 classes assigned accordingly with ranges (0- 3%, 3-15%, >15%).

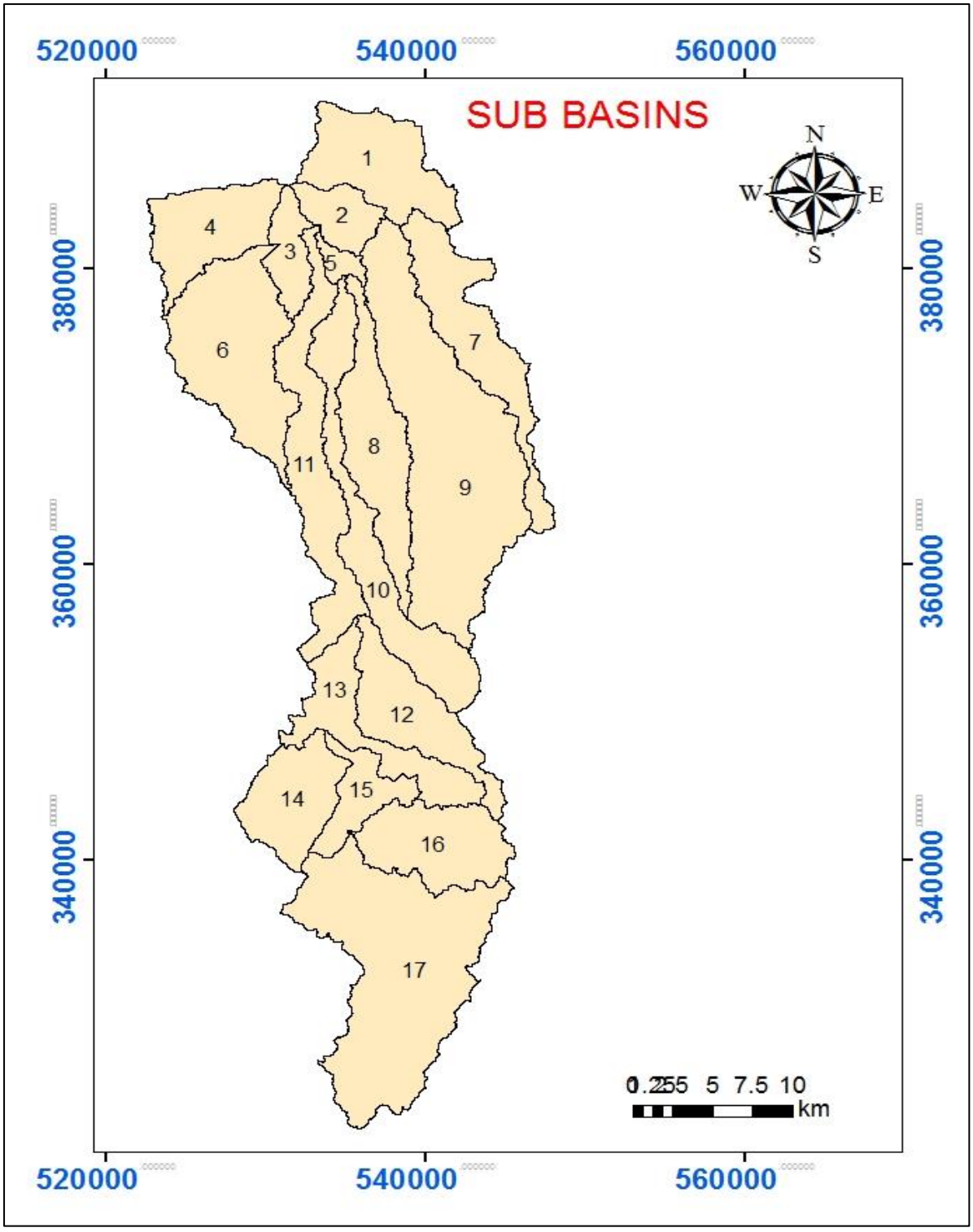

Figure 3.11: Sub basins in the watershed.

3.5.2 Writing input tables

This process involves the input of weather data in the form of tables. The weather data input into the model include: windspeed, precipitation, relative humidity, minimum and maximum temperature. The WGEN_CFSR_World was selected as the monthly weather database for filling

in any missing values. The weather generator with the help of daily precipitation, minimum and maximum temperature aids to generate the missing values Relative humidity, windspeed and solar radiation (Neitsch et al., 2011). The simulation was then activated after all required inputs, a warmup period of 3 years was used and the simulation was run for 30 years (1988-2018).

The potential evapotranspiration, was calculated by the SWAT model by the selecting the Penman Monteith method, while the curve number method was selected for the rainfall-runoff estimation.

3.6 Model simulation, calibration and validation

Calibration and validation are important aspects of any model efficiency analysis. During calibration, the most sensitive parameters of a watershed are adjusted until satisfactory results are obtained in likeness to the observed values (measured data).

Calibration of hydrologic models can either be done manually or automatically. Manual calibration involves adjustment of a parameter (s) through trial and error. One parameter or more is adjusted at a time and the results of simulated and observed values are compared to check if there is a satisfactory fitness. It is done until the modeller is satisfied with the results and this makes manual calibration a tedious process.

The SWAT model contains a 'manual calibration tool' embedded (Inchell et al., 2013). This tool provides the most dominant parameters in SWAT (in table) and enables modifications of the same. These parameters are also referred to in many other SWAT studies such as (Miller et al., 2002; Sawyer, 2010) and also in the SWAT theoretical documentation (Neitsch et al., 2011) and the SWAT Input/output Documentation (Arnold et al., 2012).

Automatic calibration employs mathematical search algorithms which check the differences between the simulated and observed (measured) values. It is a fast way of calibration, but requires a lot of expertise to employ successfully. There are a number of automatic calibration and validation tools embedded such as SWAT-CUP.

For this study, calibration was done manually according to procedure detailed in SWAT input/output documentation (Arnold et al. 2011). The table (3.7) below describes the most sensitive parameters. During the calibration, several parameters were adjusted using manual calibration tool in ArcSWAT. The model was calibrated with the available data in the period 2009-2011, while using the LULC map of 2011. This was done by adjusting a number of parameters in order to obtain a match between the simulated values and the observed values.

The Table 3.7 below summarises the most sensitive parameters adjusted by a number of researchers for various studies in relation to water balance modelling.

Table 3.7: Most sensitive SWAT parameters.

Parameter	Description	Rank
CN2	Initial SCS CN II value	1
SOL_AWC	Available soil water content	2
GW_REVAP	Groundwater "revap" coefficient	3
GWQMN	threshold depth of water in the shallow aquifer	4
ESCO	Soil evaporation compensation factor	5

Adapted from: (Abouabdillah et al., 2010; Brouziyne, Abouabdillah, Bouabid, Benaabidate, & Oueslati, 2017).

From the above selected parameters, only two were used namely CN2 and ESCO, and SOL_AWC adjusted as (0.95 CN2), (Replace 0.7), and (2 SOL_AWC) respectively.

After the calibration, model simulations were computed to assess the impacts of land-use change on water balance in the basin by using two simulation scenarios, using the same period of climatic data (01-01-1988 to 31-12-2018) and two different LULC maps 1988 (simulation1) and 2018 (simulation 2) respectively.

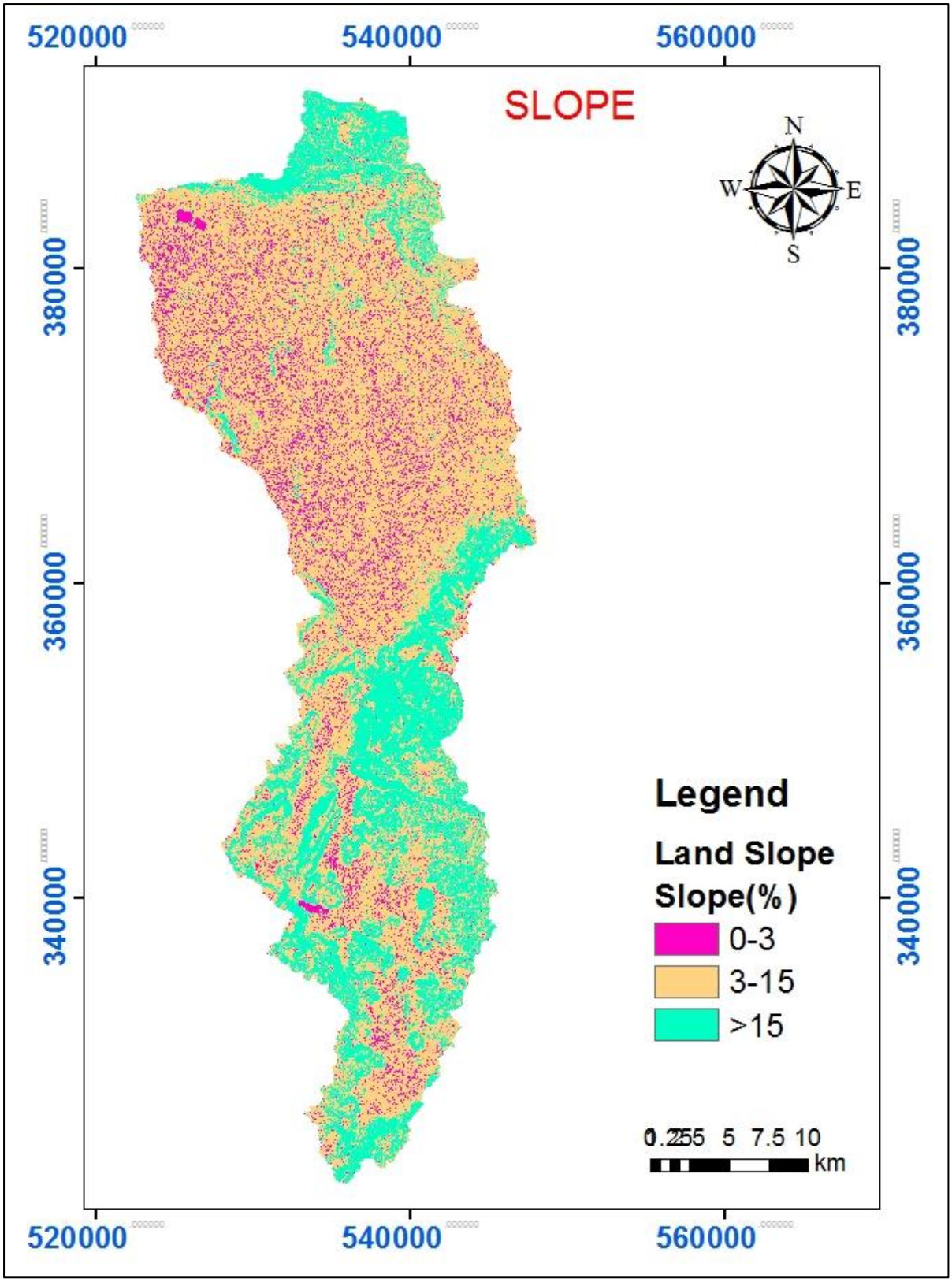

Figure 3.12: Slope map for the basin.

3.7 Performance evaluation for SWAT model

It involved use of both visual inspection and employment of statistical tools. The visual inspection involved observation of the graphs, comparing the measured and simulated flow. During visual inspection keen observation of both the peak flows and base flows is taken into consideration.

The mostly used statistical tools for evaluating hydrological models include the **Nash-Sutcliffe efficiency coefficient (NSE),** The NSE indicates how well the plot of observed versus simulated data fits the 1:1 line. Equation below is used to compute NSE.

NSE values generally range between ($-\infty \leq NSE \leq 1$), 1 being the ideal value. Whereas values ($0.0 < NSE < 1$) are acceptable for performance measures, values <0.0 indicate unacceptable, because it indicates that the mean observed value is a better predictor than the simulated value. According to Sevat and Dezetter (1991), NSE is termed the best objective function for reflecting the overall fit of a hydrograph.

$$\boldsymbol{NSE = 1 - \frac{\sum_{i=1}^{n}(Q_i - S_i)^2}{\sum_{i=1}^{n}(Q_{,i} - S_{av,i})^2}} \qquad (3.1)$$

Where:

$\boldsymbol{Q_i}$ is the observed streamflow on day i, $\boldsymbol{S_i}$ is the simulated stream flow on day i, and $\boldsymbol{S_{av,i}}$ is the average simulated stream flow on day i.

In order to measure the model performance, many researchers have used a standard set of criteria comprising a combination of numerical measures and graphical plots. Various researchers have used not only numerical measures such as Nash–Sutcliffe model efficiency, error index, and model efficiency (Choi & Deal, 2008; He & Hogue, 2011) but also graphical plots including joint plots of the simulated and observed hydrographs, scatter plots, and flow duration curves to test the model performance. Obtaining a Nash–Sutcliffe coefficient of zero indicates that model's prediction is no better than using the mean of the observed values (Choi & Deal, 2008). Different criteria assess the performance in different ways. The coefficient of efficiency (Bormann et al., 2009; Mccoll & Aggett, 2007) is used as a measure of goodness of fit, whereas the bias (He & Hogue, 2011) and are used to describe difference between simulated and observed long-term water balance.

Pearson's coefficient of determination (R^2)

This coefficient is an indicator of the strength of linear relationship between observed and simulated values.

The correlation coefficient, which ranges from −1 to 1, is an index of the degree of linear relationship between observed and simulated data. If r = 0, no linear relationship exists. If r = 1 or −1, a perfect positive or negative linear relationship exists. Similarly, R^2 describes the proportion of the variance in measured data explained by the model. R^2 ranges from 0 to 1, with higher values indicating less error variance, and typically values greater than 0.5 are considered acceptable (Liew & Garbrecht, 2003; Santhi et al., 2002). Although r and R2 have been widely used for model evaluation, these statistics are oversensitive to high extreme values (outliers) and insensitive to additive and proportional differences between model predictions and measured data (Legates and McCabe, 1999).

$$\boldsymbol{R^2} = \left(\frac{\sum_i^n (\boldsymbol{Q_{,i}} - \boldsymbol{Q_{av,i}}) \times (\boldsymbol{S_i} - \boldsymbol{S_{av,i}})}{\left[\sum_i^n (\boldsymbol{Q_i} - \boldsymbol{Q_{av,i}})^2 \times \sum_i^n (\boldsymbol{S_i} - \boldsymbol{S_{av,i}})^2 \right]^{0.5}} \right)^{\mathbf{2}} \quad (3.2)$$

Where:

$\boldsymbol{Q_{,i}}$ is the observed streamflow on day i, $\boldsymbol{S_i}$ is the simulated stream flow on day i, $\boldsymbol{Q_{av,i}}$ is the mean observed streamflow on day i, and $\boldsymbol{S_{av,i}}$ is the average simulated stream flow on day i.

Percent bias (PBIAS):

PBIAS measures the deviation of the simulated values from the observed values (Gupta et al., 1999). PBIAS equals zero is the ideal value. While low values of PBIAS imply accurate model simulations, positive values imply an underestimation bias, negative values imply an over estimation bias (Gupta et al., 1999). Expressed as a percentage, PBIAS can be estimated from equation 3.3 below.

$$\boldsymbol{PBIAS} = \frac{\sum_i^n (\boldsymbol{Q_{,i}} - \boldsymbol{S_i})}{\sum_i^n \boldsymbol{Q_{,i}}} \quad (3.3)$$

Where:

$\boldsymbol{Q_{,i}}$ is the observed streamflow on day i, $\boldsymbol{S_i}$ is the simulated stream flow on day i, while n is the total number of years.

The table below entails the statistical criterion of the selected parameters, values are based on literature review (Moriasi et al., 2007).

Table 3.8: Statistical criterion.

Performance Criterion	Value	Indication
Nash-Sutcliffe coefficient	$0.75 < NSE \leq 1.00$	Very good
	$0.65 < NSE \leq 0.75$	Good
	$0.50 < NSE \leq 0.65$	Satisfactory
	$0.40 < NSE \leq 0.50$	Acceptable
	$NSE \leq 0.4$	Unsatisfactory
	$0.40 \leq NSE \leq 0.70$	Acceptable
Percent bias	$PBIAS < \pm 10$	Very good
	$\pm 10 \leq PBIAS < \pm 15$	Good
	$\pm 15 \leq PBIAS < \pm 25$	Satisfactory
	$PBIAS \geq \pm 25$	Unsatisfactory

CHAPTER FOUR

RESULTS AND DISCUSSIONS

4 Land use Land cover analysis

The land use maps for 2018 and 1988 shown in figures 4.1 and 4.2 both indicate that the dominant land use type is arable lands for both periods. Visible changes are observed in the increase in urban land, arboriculture, water, and irrigated agriculture and a reduction in range lands, forests and arable lands.

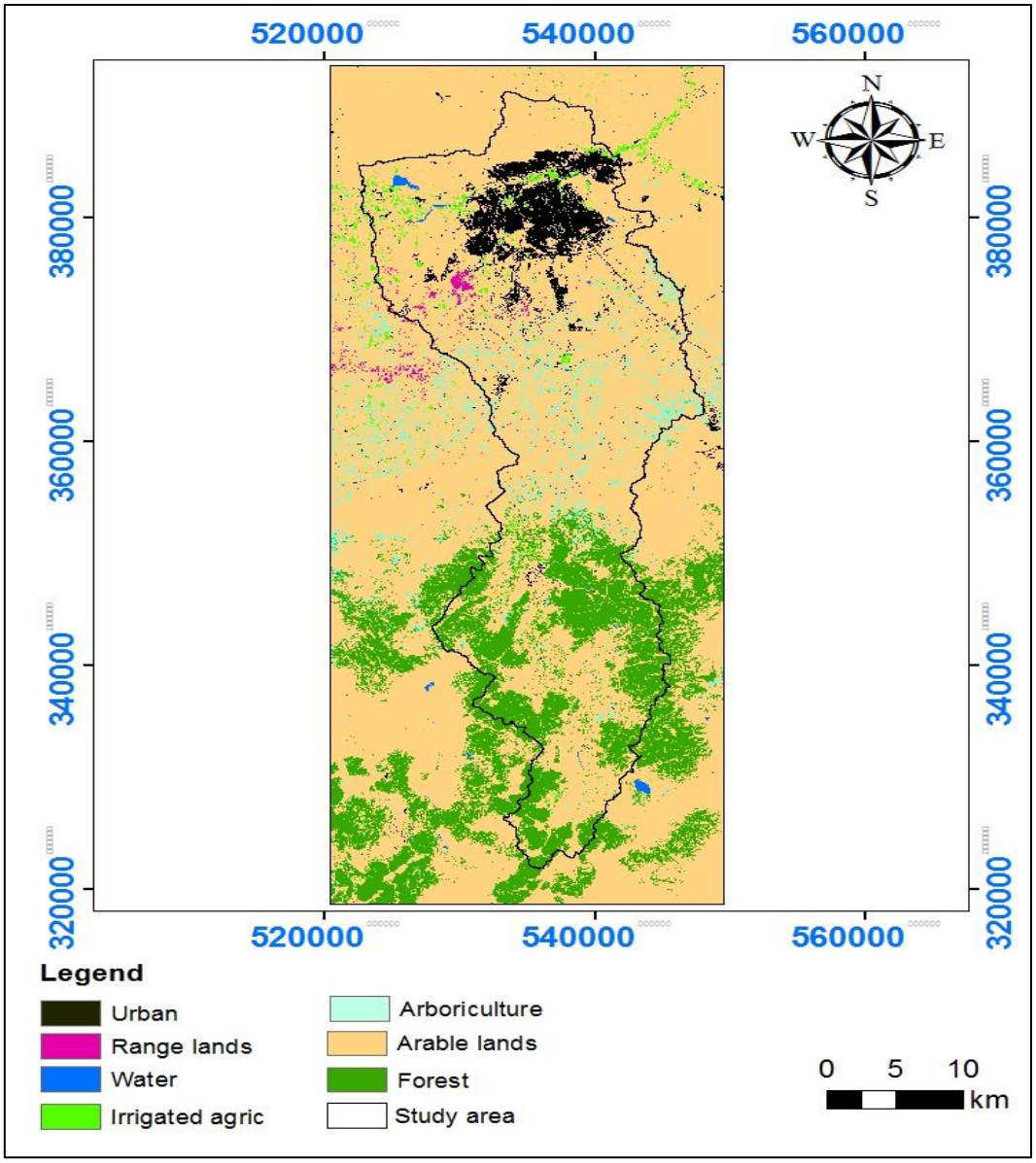

Figure 4.1: Land-use classification map for 2018

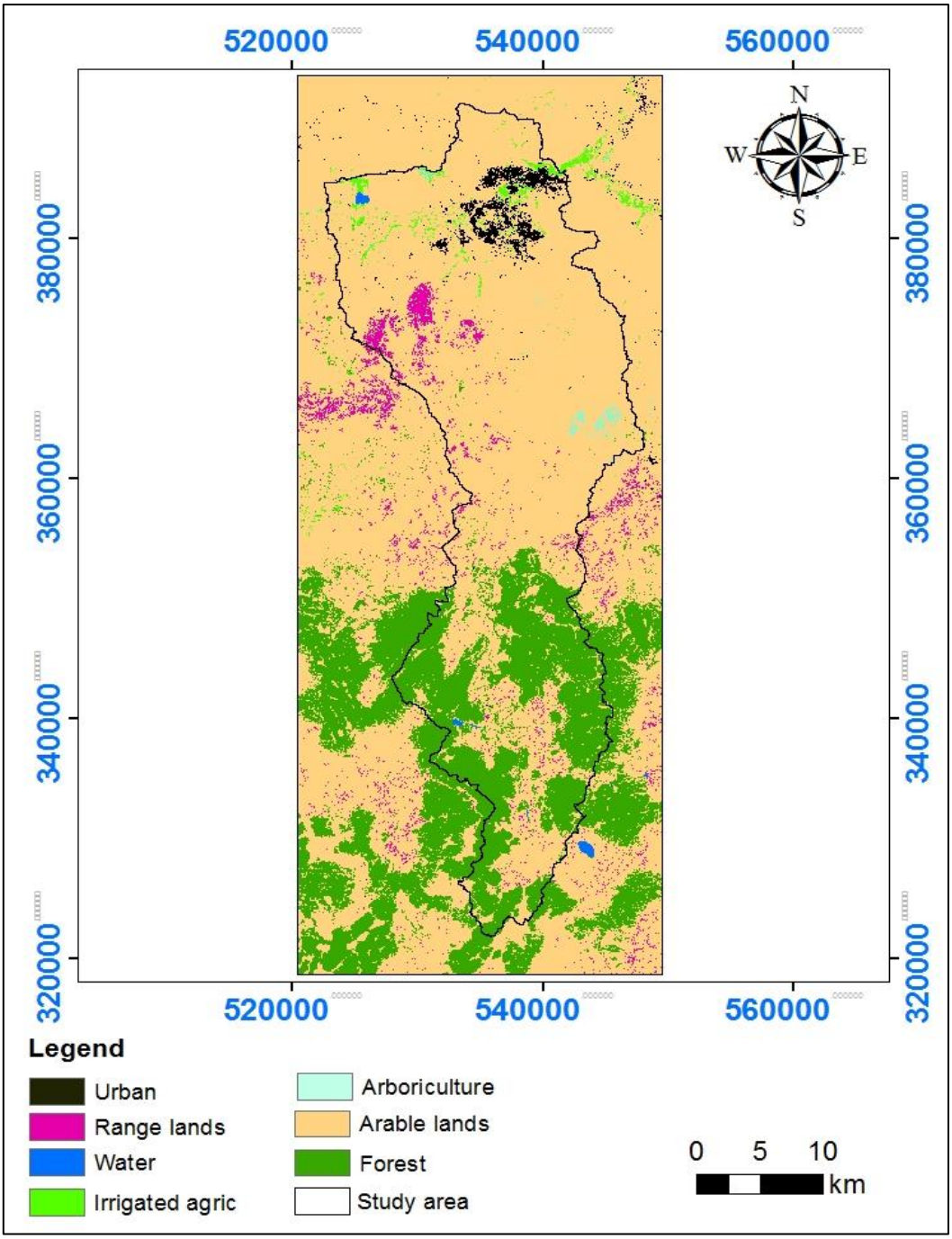

Figure 4.2: Land use classification map for 1988.

4.1.1 Accuracy assessment and validation

The confusion matrix for land use assessment 1988 and 2018 are shown in tables 4.1 and 4.2 respectively.

For the accuracy assessment of 1988 land use classification, the overall accuracy obtained from the random sampling process for the image was 92.61%. User's accuracy ranged from 80% to 100% while producer's accuracy ranged from 57.14% to 100%. The wide range of accuracy

indicates a severe confusion of arable land with other land cover classes, and a confusion of forests with arable lands. The user's accuracy clearly indicates the classification of each land cover class as is actually depicted on ground. Water and irrigated agriculture were both correctly classified with 100% accuracy is this is because both classes had a small representation in the total classification which made it easy to correctly indicate.

The commission error reflects the pixels which are included in another class to which they do not belong. While arable lands is expected to have the highest commission error due to the many numbers of pixels classified as other classes, arboriculture instead has the highest commission error and this is due to the small number of total pixels (14) compared with 253 total of arable land. Arboriculture has a commission error of (0.2)

Likewise, the omission error shows the number of pixels which are not included in the class to which they really belong. Irrigated agriculture and arboriculture have the highest omission error (0.429), with 3(out of 7) points for agriculture and 6 (out of 14) points for arboriculture not being categorized in these classes.

For the accuracy assessment of 2018 land use classification, the overall accuracy obtained from the random sampling process for the image was 92%. User's accuracy ranged from 75% to 100% while producer's accuracy ranged from 35.29% to 100%. Similar to the 1988 assessment, a severe confusion of arable land with other land cover classes, and a confusion of forests with arable lands was noted. Water and range lands were both correctly classified with 100% user's accuracy is this is because of the ease of identification of these classes.

The omission error for arboriculture was the highest (0.647), with 11(out of 17) pixels for arboriculture being categorized as arable lands.

Tables 4.1 and 4.2 below show the error matrix for land use classification for 1988 and 2018 respectively. The Kappa index for 1988 and 2018 was 0.85 and 0.842 respectively. Both assessment results were satisfactory and within acceptable ranges refer to (Table 3.2)

Table 4.1: Error matrix accuracy assessment for 1988

Class	Water	Irrigated land	Forests	Arable lands	Range lands	Arboriculture	Urban	User total	User's accuracy	Commission error
Water	3.00	0.00	0.00	0.00	0.00	0.00	0.00	3.00	100.00	0.00
Irrigated land	0.00	4.00	0.00	0.00	0.00	0.00	0.00	4.00	100.00	0.00
Forests	0.00	0.00	61.00	5.00	0.00	0.00	0.00	66.00	92.42	7.58
Arable lands	0.00	3.00	4.00	244.00	6.00	6.00	0.00	263.00	92.78	7.22
Rangelands	0.00	0.00	0.00	1.00	10.00	0.00	0.00	11.00	90.91	9.09
Arboriculture	0.00	0.00	0.00	2.00	0.00	8	0.00	10.00	80.00	20.00
Urban	0.00	0.00	0.00	1.00	0.00	0.00	21.00	22.00	95.45	4.55
Producer total	3.00	7.00	65.00	253.00	16.00	14.00	21.00	**379.00**		
Producer accuracy	100.00	57.14	93.85	96.44	62.50	57.14	100.00			
Omission error	0.00	42.86	6.15	3.56	37.50	42.86	0.00			

Table 4.2: Error matrix accuracy assessment for 2018.

Class	Irrigated agriculture	Range lands	Arable lands	Urban	Water	Forest	Arboriculture	User total	User's accuracy	Commission error
Irrigated agriculture	9.00	0.00	1.00	0.00	0.00	0.00	0.00	10.00	90.00	10.00
Range lands	0.00	6.00	0.00	0.00	0.00	0.00	0.00	6.00	100.00	0.00
Arable lands	2.00	0.00	232.00	0.00	0.00	5.00	11.00	250.00	92.80	7.20
Urban	0.00	0.00	1.00	37.00	0.00	0.00	0.00	38.00	97.37	2.63
Water	0.00	0.00	0.00	0.00	4.00	0.00	0.00	4.00	100.00	0.00
Forest	0.00	0.00	7.00	0.00	0.00	39	0.00	46.00	84.78	15.22
Arboriculture	0.00	0.00	1.00	0.00	0.00	1.00	6.00	8.00	75.00	25.00
Producer total	11.00	6.00	242.00	37.00	4.00	45.00	17.00	362.00		
Producer accuracy	81.82	100.00	95.87	100.00	100.00	86.67	75.00			
Omission error	0.00	0.00	4.13	0.00	0.00	13.33	64.71			

4.1.2 Land use/cover change detection and analysis

For this study the cross tabulation involves the calculation of area per land cover class using ArcGIS 10.3 and the calculation of changes in the various land covers by area percentage between the study period of 1988 and 2018. The results from the land-use classification are summarised in Table 4.3.

From the classification of 1988, arable lands were the dominant land use type with an area of (649.62 km^2), followed by: forests (193.23 km^2), range lands (22.13 km^2), Urban (20.49 km^2), Irrigated fields (10.40 km^2), arboriculture (3.49 km^2), and water (1.37 km^2) respectively. Similarly, for the LULC classification for 2018, Arable lands is still the dominant type (611.37 km^2), followed by: forests (154.85 km^2), Urban (75.08 km^2), arboriculture (36.44 km^2), irrigated agriculture (15.71 km^2), range lands (5.10 km^2), and water (2.17 km^2), respectively.

Numerous changes were observed in all land use classes, the biggest changes occurring for range lands, urban, arboriculture, water and irrigated agriculture respectively. Minor changes were observed for arable lands and forests.

Table 4.3: Area of land use 1988 and 2018.

Class name	1988		2018		(2018-1988)	
	Area (km^2)	Area (%)	Area (km^2)	Area (%)	Variation (km^2)	% Change
Urban	20.49	2.27	75.08	8.34	54.59	72.71
Range lands	22.13	2.46	5.10	0.57	-17.02	-333.62
Water	1.37	0.15	2.17	0.24	0.80	36.85
Arboriculture	3.49	0.39	36.44	4.05	32.95	90.43
Forest	193.23	21.45	154.85	17.19	-38.39	-24.79
Arable lands	649.62	72.12	611.37	67.88	-38.24	-6.26
Irrigated agriculture	10.40	1.15	15.71	1.74	5.31	33.78

The results from figure 4.3 further indicate a percentage variation in the different land uses, with an increase in urban by (72.71%), arboriculture by (90.43%), water by (36.855), and irrigated agriculture by (33.78%), a significant decrease in arable lands by (6.26%), forests by (24.79%), and range lands by (333.62%). The increase in water area is as a result of the increased irrigated agriculture practices over the past 30 years since 1988.

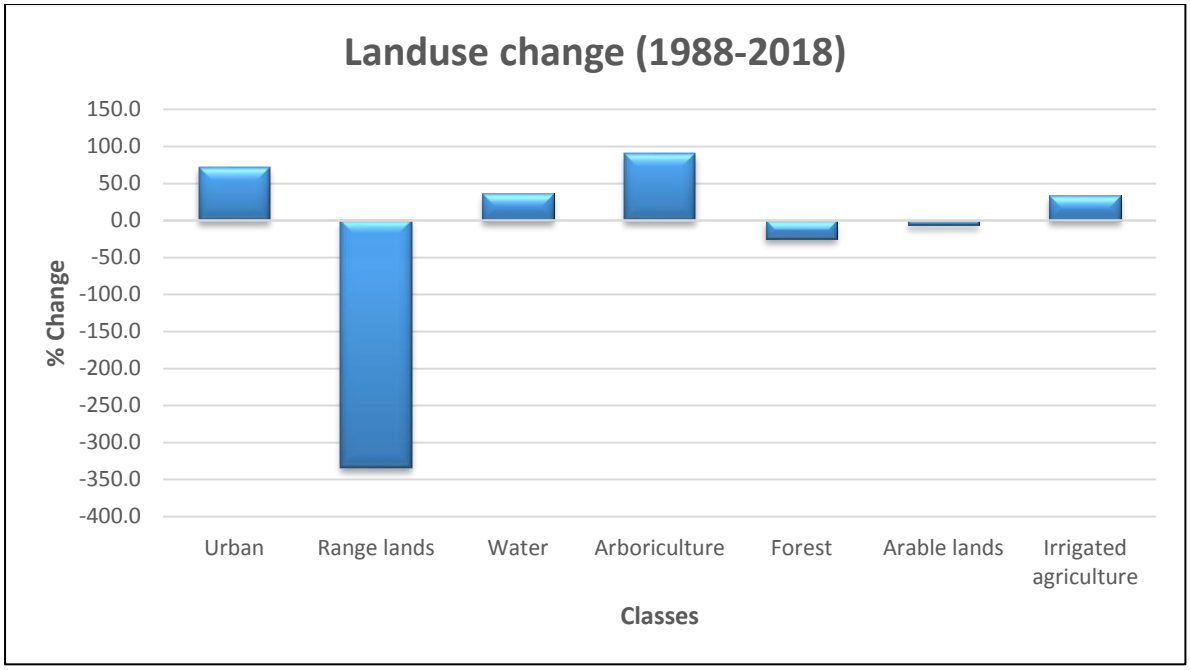

Figure 4.3: Variation in land-use between 1988 and 2018.

4.2 Model simulation

To establish the impact of change in land use on hydrologic components the simulation period has been divided into two periods: i) the first period (2003–2018) for which 2018 land-use layer has been employed for calibration, ii) the second period (1984–2000) for which 1988 land-use layer has been employed for validation.

4.2.1 Calibration and validation

The model was calibrated with data from 9-June-2009 to 06-Dec-2011 as (random points daily measurements), and since the calibration process modelled the water balance components close to actual values, a validation assumption was made with no further adjustments and comparisons. The initial calibration involved the balancing of the long-term annual water balance components including total water yield, evapotranspiration, PET and Rainfall. The annual average rainfall for calibration period (2009-2011) was 708mm, PET was 1011.4 mm, Total water yield (TWYLD) 232.51 mm, surface runoff was 113.64mm, and ET was 482.1 mm. The calibration of the stream flow was then conducted by adjusting the initial SCS run-off curve number (CN2), and soil evaporative compensation factor (ESCO) and available water content (SOL_AWC). Figure 4.4, shows calibrated results of the daily discharge of the basin. The simulated results for calibration mostly indicate an under estimation of the simulated stream flow in comparison to the observed values. This under estimation is explained by the large change of land-use, complexities of the model, and the lack of having actual data regarding the soil properties.

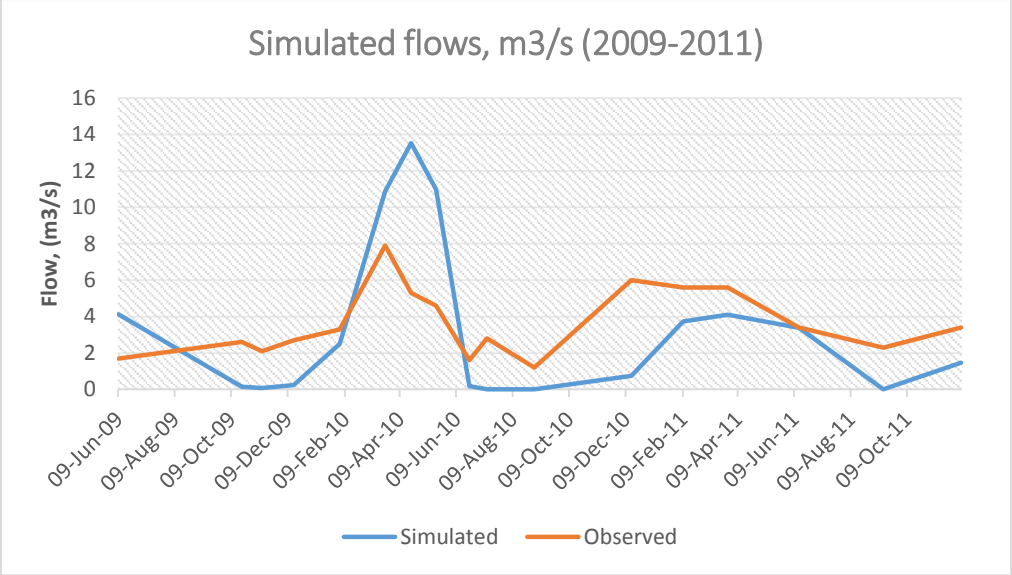

Figure 4.4: daily simulated and observed flow values during calibration period (2009-2011).

The calibrated values were used to validate the land cover map of 1988. The validation was done by using the land use map of 1988 and climate data for the period (1984-2000). The calibrated parametres were used during the simulations and all values were assumed to be in agreement since the calibartion parameters were in agreement.

4.3 Impacts of LULC on water balance

The long-term annual values of water balance components for the two simulation periods using LULC 1988, LULC 2018 and same climatic data for the period (1988-2018)

Table 4.4: long term annual average water balance components for land use simulations, with climate data (1988-2018) and Land-use data for 1988 & 2018.

LULC data	PCP (mm)	Total water yield (mm)	ET (mm)	Surface runoff (mm)	Lateral flow (mm)	GW Shall AQ (mm)	GW Deep AQ (mm)
1988	426.6	132.08	275.9	89.93	8.15	31.33	2.66
2018	426.6	133.69	274.7	94.76	8.03	28.41	2.41
% Change		1.20	-0.44	5.10	-1.49	-10.28	-10.37

The effects of changes in land use & land cover on the different hydrologic components, particularly runoff, ET and base flow (ground water shallow aquifer and deep aquifer) in Oued Fez basin were analysed on both annual and monthly time scale. In order to assess the impacts of LULC changes on hydrological water balance, two separate simulations of the SWAT model were performed using LULC maps of 1988 and 2018, respectively and same climatic data for period (1988-2018).

The impact of LULC on water balance between the period 1988 and 2018 indicates the variations of the percentage of rainfall that contributes to the various water balance components in the basin. The ratios of water balance components in relation to annual precipitation indicate 64.67% ET, surface runoff represents 21.08%, and lateral flow is 1.91% of annual precipitation, Groundwater deep aquifer is 0.62% while groundwater shallow aquifer is 7.34% for scenario 1 (using LULC map 1988)

Similarly, using the LULC map of 2018 evapotranspiration is 64.39% of annual precipitation, while 22.21% of PRECP is surface runoff, and lateral flow is 1.88% , ground water deep aquifer is 0.56% while groundwater shallow aquifer is 6.65% as calculated from table 4.4. The water balance in both scenarios is majorly dominated by actual evapotranspiration.

The changes in LULC impacted on the water balance in the Oued Fez basin. The annual average surface runoff increased from 89.93mm in 1988, to 94.76 mm in 2018 and this increase can be explained by the slight increase in urban area in 2018 are a higher contributing factor to this. The ground water shallow aquifer reduced from 31.33mm in 1988 to 28.41 mm in 2018. The reduction in the component of ground water is in alignment with the research reported by (Legrouri et al., 2012), indicating the declining levels of the water in shallow aquifer. The percentage changes in the various water balance components in the basin indicate an increase in the; total water yield by 1.20%, and surface runoff by 5.10%, reductions were also noted for: ET by 0.44%, lateral flow by 1.49%, ground water in shallow aquifer by 10.28%, and groundwater deep aquifer by 10.37%.

Additionally results from simulations further indicate that the land uses which had a major impact on the water balance components include: forests, arable lands, irrigated agriculture, and arboriculture for simulations under the LULC map of 2018, while for the simulations of LULC 1988, range lands, arable lands, and forests were the dominating land-uses with a greater influence on the water balance.

The average monthly basin values for periods with climatic data for the period (1988-2018) LULC maps for 1988 and 2018 are summarised in tables 4.5 and 4.6 respectively. The increases in the monthly basin values between 1988 and 2018 is attributed to the various changes in the LULC in the basin.

Table 4.5: Average monthly basin values for the period (1988-2018) and LULC 1988.

Month	Rain (mm)	Snow (mm)	Surface Runoff (mm)	Lateral flow (mm)	Water yield (mm)	ET (mm)	PET(mm)
1	59.61	0.5	16.03	1.21	20.22	14.23	24.63
2	48.58	0.02	11.93	1.12	18.65	19.48	35.47
3	53.76	0	16.73	1.18	26.39	29.97	63.69
4	48.61	0	12.59	0.93	21.21	36.01	83.26
5	28.05	0	5.55	0.69	11.5	49.68	112.14
6	8.61	0	0.5	0.37	2.67	59.11	138.61
7	0.81	0	0	0.19	0.62	19.96	167.02
8	3.28	0	0.06	0.12	0.38	4.56	152.06
9	15.03	0	0.34	0.13	0.61	6.51	101.97
10	41.97	0	2.52	0.36	2.95	12.98	63.63
11	62.01	0	10.54	0.74	11.15	12.12	32.2
12	55.8	0	13.04	1.1	15.56	11.14	21.5
Annual totals	426.12	0.52	89.83	8.14	131.91	275.75	996.18

The average monthly basin values also varied from one month to another between two simulation scenarios. The values not only increased on average monthly basis but also on sub basin level.

Table 4.6: Average monthly basin values for the period (1988-2018) and LULC 2018.

Month	Rain (mm)	Snow (mm)	Surface Runoff (mm)	Lateral flow (mm)	Water yield (mm)	ET (mm)	PET(mm)
1	59.61	0.5	16.66	1.2	20.53	14.24	24.63
2	48.58	0.02	12.46	1.1	18.64	19.47	35.47
3	53.76	0	17.3	1.16	26.24	30.05	63.69
4	48.61	0	13.13	0.92	21.06	36.81	83.26
5	28.05	0	5.83	0.67	11.26	50.69	112.14
6	8.61	0	0.56	0.37	2.54	57.93	138.61
7	0.81	0	0	0.19	0.57	18.35	167.02
8	3.28	0	0.08	0.11	0.38	4.38	152.06
9	15.03	0	0.5	0.13	0.75	6.49	101.97
10	41.97	0	3.06	0.36	3.48	12.93	63.63
11	62.01	0	11.43	0.73	12.04	12.09	32.2
12	55.8	0	13.64	1.09	16.02	11.13	21.5
Annual totals	426.12	0.52	94.65	8.03	133.51	274.56	996.18

4.4 Evaluation of model efficiency

The model was evaluated using three statistical tools namely, PBIAS, NSE and coefficient of determination. The statistics were computed for the calibration period and the evaluation of model efficiency for the various statistical tools was computed by comparing the simulated flow values and the observed flow values.

An NSE value of -2.45, PBIAS 9.70 and R^2 of 0.421 were obtained during the calibration period. The negative NSE value is outside the acceptable range and this value indicates a model underestimation, the PBIAS and R^2 values are with acceptable ranges, according to table 3.8. The scatter plot in figure 4.5 indicates the goodness of fit using R^2. The model performance was not satisfactory given the results obtained from the statistical evaluation.

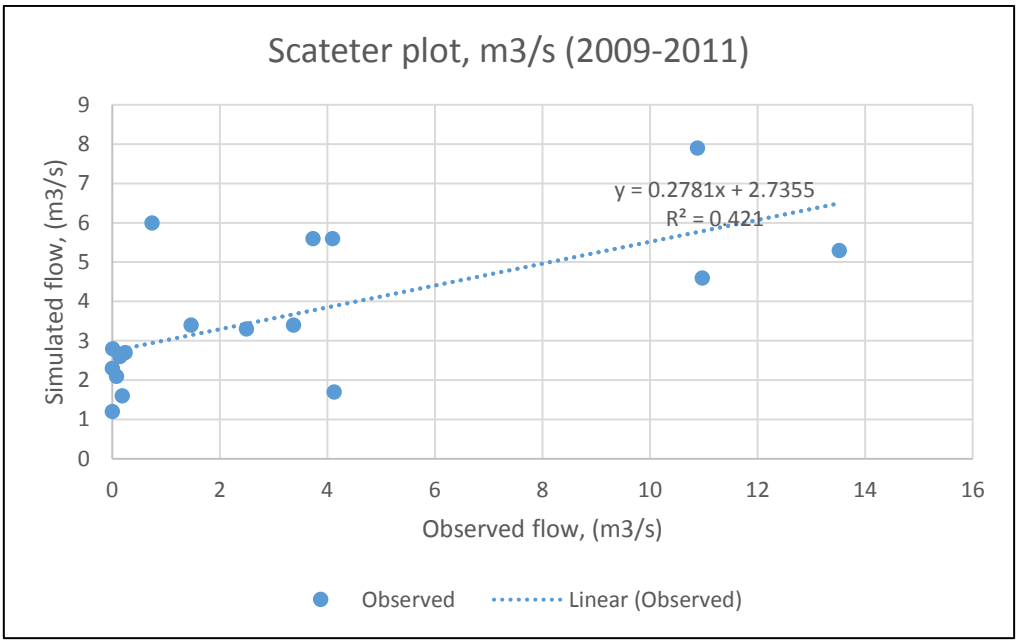

Figure 4.5: Scatter plot for observed versus simulated flow during calibration period (2009-2011).

CONCLUSION AND RECOMMENDATIONS

Conclusion

The SWAT model requires a lot of input data, and utmost accuracy is required during the data collection in order to obtain precise information for hydrological modelling. Therefore, to ensure collection of accurate and precise information various data sources were used for different data inputs like described in the methodology.

This study's main focus was to simulate the impacts of land-use change on water balance and hydrology in the Oued Fez basin, an area which has undergone tremendous land use changes for the past 30 years from 1988 to 2018. The SWAT model was used to assess the hydrological impacts, using two LULC maps (1988 and 2018) respectively and thus the results obtained from the two scenarios were compared to check the evolution of water balance in the basin.

Significant changes in land-use were observed between 1988 and 2018, with the biggest land-use conversion being the reduction in range lands by (333.62%), and increase in arboriculture, urban, and irrigated agriculture by (90.43%), (72.71%), and (33.78%) respectively. The surface water also notably increased by (36.85%) and this is attributed the increase in irrigated agriculture practices, the construction of two dams after the year 1988.

The simulation of land-use changes indicated considerable changes in water balance components. The changes in land use land cover, greatly impacted on the changes on water balance and stream flow in the Oued Fez basin, which indicated an increase in annual average values: surface runoff increased from 89.93mm in 1988, to 94.76 mm in 2018 and this increase can be explained by the slight increase in urban area in 2018 are a higher contributing factor to this. The ground water shallow aquifer reduced from 31.33mm in 1988 to 28.41 mm in 2018. The reduction in the component of ground water is in alignment with the research reported by (Legrouri et al., 2012), indicating the declining levels of the water in shallow aquifer. The percentage changes in the various water balance components in the basin indicate an increase in the; total water yield by 1.20%, and surface runoff by 5.10%, reductions were also noted for: ET by 0.44%, lateral flow by 1.49%, ground water in shallow aquifer by 10.28%, and groundwater deep aquifer by 10.37%.

Additionally results from simulations further indicate that the land uses which had a major impact on the water balance components include: forests, arable lands, irrigated agriculture, and arboriculture for simulations under the LULC map of 2018, while for the simulations of

LULC 1988, range lands, arable lands, and forests were the dominating land-uses with a greater influence on the water balance.

Recommendations

For efficient optimization of the SWAT model, input data in regards to surface storage, water impoundments should be considered and accounted for in the model in order to obtain better results.

It is recommended that further studies be conducted to assess the relationship between aquifer over pumping and flooding in relation to land-use changes.

REFERENCES

ABHS (Agence de Bassin Hydraulique de Sebou), (2004). Synthèse hydrogéologique du bassin Fès-Meknès. Rapport de la mission II, 90 p.

ABHS, (Agence de Bassin Hydraulique de Sebou), (2006). Evaluation des ressources en eau souterraines de la nappe de Fès-Meknès. Rapport de la mission I, 50 p.

Abdollahi, K., Bazargan, A., & McKay, G. (2019). Water Balance Models in Environmental Modeling. *Handbook of Environmental Materials Management*, (January), 1961–1976. https://doi.org/10.1007/978-3-319-73645-7_119

Abouabdillah, A., Oueslati, O., De Girolamo, A. M., & Lo Porto, A. (2010). Modeling the impact of climate change in a mediterranean catchment (Merguellil, Tunisia). *Fresenius Environmental Bulletin*, *19*(10 A), 2334–2347.

Adhikari, R. K., Mohanasundaram, S., & Shrestha, S. (2020). Impacts of land-use changes on the groundwater recharge in the Ho Chi Minh city , Vietnam. *Environmental Research*, *185*(February), 109440. https://doi.org/10.1016/j.envres.2020.109440

Aduah, M. S., Jewitt, G. P. W., & Toucher, M. L. W. (2017). Assessing impacts of land use changes on the hydrology of a lowland rainforest catchment in Ghana, West Africa. *Water (Switzerland)*, *10*(1). https://doi.org/10.3390/w10010009

Ahiablame, L., Sinha, T., Paul, M., Ji, J. H., & Rajib, A. (2017). Streamflow response to potential land use and climate changes in the James River watershed, Upper Midwest United States. *Journal of Hydrology: Regional Studies*, *14*(November), 150–166. https://doi.org/10.1016/j.ejrh.2017.11.004

Anil, A. P., & Ramesh, H. (2017). Analysis of climate trend and effect of land use land cover change on Harangi streamflow, South India: a case study. *Sustainable Water Resources Management*, *3*(3), 257–267. https://doi.org/10.1007/s40899-017-0088-5

Arnold, J G, Srinivasan, R., Muttiah, R. S., & Williams, J. R. (1998). *LARGE AREA HYDROLOGIC MODELING AND ASSESSMENT PART I : MODEL DEVELOPMENT ' basin scale model called SWAT (Soil and Water speed and storage , advanced software debugging policy to meet the needs , and the management to the tank model (Sugawara et al ., 1*. *34*(1), 73–89.

Arnold, Jeffrey G., Allen, P. M., & Bernhardt, G. (1993). A comprehensive surface-

groundwater flow model. *Journal of Hydrology*, *142*(1–4), 47–69. https://doi.org/10.1016/0022-1694(93)90004-S

Awotwi, A. (2009). Detection of land use and land cover change in Accra, Ghana, between 1985 and 2003 using Landsat Imagery. Master Thesis, Royal Institute of Technology (KTH)., Division of Geoinformatics.

Bai, Y., Feng, M., Jiang, H., Wang, J., & Liu, Y. (2015). Validation of land cover maps in China using a sampling-based labeling approach. *Remote Sensing*, *7*(8), 10589–10606. https://doi.org/10.3390/rs70810589

Batelaan, O., & De Smedt, F. (2001). WetSpass: A flexible, GIS based, distributed recharge methodology for regional groundwater modelling. *IAHS-AISH Publication*, (269), 11–18.

Bhaduri, B., Harbor, J., Engel, B., & Grove, M. (2000). Assessing watershed-scale, long-term hydrologic impacts of land-use change using a GIS-NPS model. *Environmental Management*, *26*(6), 643–658. https://doi.org/10.1007/s002670010122

Bormann, H., Breuer, L., & Gra, T. (2009). *Assessing the impact of land use change on hydrology by ensemble modelling (LUCHEM) IV : Model sensitivity to data aggregation and spatial (re-) distribution*. *32*, 171–192. https://doi.org/10.1016/j.advwatres.2008.01.002

Bouabid, R., & Elalaoui, A. C. (2010). *Impact of climate change on water resources in Morocco : The case of Sebou Basin I – Introduction*. *62*, 57–62.

Briak, H., Moussadek, R., Aboumaria, K., & Mrabet, R. (2016). Assessing sediment yield in Kalaya gauged watershed (Northern Morocco) using GIS and SWAT model. *International Soil and Water Conservation Research*, *4*(3), 177–185. https://doi.org/10.1016/j.iswcr.2016.08.002

Brouziyne, Y., Abouabdillah, A., Bouabid, R., Benaabidate, L., & Oueslati, O. (2017). SWAT manual calibration and parameters sensitivity analysis in a semi-arid watershed in North-western Morocco. *Arabian Journal of Geosciences*, *10*(19). https://doi.org/10.1007/s12517-017-3220-9

Brown, A. E., Zhang, L., McMahon, T. A., Western, A. W., & Vertessy, R. A. (2005). A review of paired catchment studies for determining changes in water yield resulting from

alterations in vegetation. *Journal of Hydrology*, *310*(1–4), 28–61. https://doi.org/10.1016/j.jhydrol.2004.12.010

Chadli, K., Kirat, M., Laadoua, A., & El Harchaoui, N. (2016). Runoff modeling of Sebou watershed (Morocco) using SCS curve number method and geographic information system. *Modeling Earth Systems and Environment*, *2*(3), 1–8. https://doi.org/10.1007/s40808-016-0215-6

Chaikaew, P. (2019). Land Use Change Monitoring and Modelling using GIS and Remote Sensing Data for Watershed Scale in Thailand. *Land Use - Assessing the Past, Envisioning the Future*. https://doi.org/10.5772/intechopen.79167

Chander Gyanesh, Brian L. Markham, D. L. H. (2009). Remote Sensing of Environment Summary of current radiometric calibration coef fi cients for Landsat MSS , TM , ETM + , and EO-1 ALI sensors. *Remote Sensing of Environment*, *113*(5), 893–903. https://doi.org/10.1016/j.rse.2009.01.007

Choi, W., & Deal, B. M. (2008). *Assessing hydrological impact of potential land use change through hydrological and land use change modeling for the Kishwaukee River basin (USA). 88*, 1119–1130. https://doi.org/10.1016/j.jenvman.2007.06.001

Chu, H. J., Lin, Y. P., Huang, C. W., Hsu, C. Y., & Chen, H. Y. (2010). Modelling the hydrologic effects of dynamic land-use change using a distributed hydrologic model and a spatial land-use allocation model. *Hydrological Processes*, *24*(18), 2538–2554. https://doi.org/10.1002/hyp.7667

Clifton, C. F., Day, K. T., Luce, C. H., Grant, G. E., Safeeq, M., Halofsky, J. E., & Staab, B. P. (2018). E ff ects of climate change on hydrology and water resources in the Blue. *Climate Services*, (October 2017), 0–1. https://doi.org/10.1016/j.cliser.2018.03.001

Collins, F., Division, E. S., Ridge, O., Ridge, O., Group, R., Sciences, A., … Group, S. (2002). *The influence of land-use change and landscape dynamics on the climate system : relevance to climate-change policy beyond the radiative e ® ect of greenhouse gases*. 1705–1719.

Denizman, C. (2018). Land use changes and groundwater quality in Florida. *Applied Water Science*, *8*(5), 1–17. https://doi.org/10.1007/s13201-018-0776-9

Devia, G. K., Ganasri, B. P., & Dwarakish, G. S. (2015). A Review on Hydrological Models.

Aquatic Procedia, *4*(Icwrcoe), 1001–1007. https://doi.org/10.1016/j.aqpro.2015.02.126

Dwarakish, G. S., & Ganasri, B. P. (2015). Impact of land use change on hydrological systems: A review of current modeling approaches. *Cogent Geoscience*, *1*(1), 1–18. https://doi.org/10.1080/23312041.2015.1115691

El, A., Mulla, D. J., El, S., & Knight, J. (2017). Analysis of urban growth and sprawl from remote sensing data : Case of Fez , Morocco. *International Journal of Sustainable Built Environment*. https://doi.org/10.1016/j.ijsbe.2017.02.003

Faculty, U. U. N. L., Liew, M. W. Van, Bosch, D. D., & Arnold, J. G. (2007). *DigitalCommons @ University of Nebraska - Lincoln Suitability of SWAT for the Conservation Effects Assessment Project : Comparison on USDA Agricultural Research Service Watersheds Suitability of SWAT for the Conservation Effects Assessment Project : Comparison on USDA Agricultural Research*.

Fohrer, N., Haverkamp, S., Eckhardt, K., & Frede, H. G. (2001). Hydrologic response to land use changes on the catchment scale. *Physics and Chemistry of the Earth, Part B: Hydrology, Oceans and Atmosphere*, *26*(7–8), 577–582. https://doi.org/10.1016/S1464-1909(01)00052-1

Foody, G. (2010). Assessing the Accuracy of Remotely Sensed Data: Principles and Practices. In *The Photogrammetric Record* (Vol. 25). https://doi.org/10.1111/j.1477-9730.2010.00574_2.x

Foody, G. M. (2002). Status of land cover classification accuracy assessment. *Remote Sensing of Environment*, *80*(1), 185–201. https://doi.org/10.1016/S0034-4257(01)00295-4

Francoise, Molle,Tanouti, O. (2017). *Squaring the circle : Agricultural intensification vs . water conservation in Morocco*. *192*, 170–179. https://doi.org/10.1016/j.agwat.2017.07.009

Gamo, M., Shinoda, M., & Maeda, T. (2013). Classification of arid lands, including soil degradation and irrigated areas, based on vegetation and aridity indices. *International Journal of Remote Sensing*, *34*(19), 6701–6722. https://doi.org/10.1080/01431161.2013.805281

He, M., & Hogue, T. S. (2011). *Integrating hydrologic modeling and land use projections for*

evaluation of hydrologic response and regional water supply impacts in semi-arid environments. https://doi.org/10.1007/s12665-011-1144-3

Hu, Q., Willson, G. D., Chen, X., & Akyuz, A. (2005). *Effects of climate and landcover change on stream discharge in the Ozark Highlands , USA ∗*. 9–19. https://doi.org/10.1007/s10666-004-4266-0

Hua, A. K. (2017). Land Use Land Cover Changes in Detection of Water Quality: A Study Based on Remote Sensing and Multivariate Statistics. *Journal of Environmental and Public Health*, *2017*, 5–7. https://doi.org/10.1155/2017/7515130

Johnson, T., Butcher, J., Deb, D., Faizullabhoy, M., Hummel, P., Kittle, J., … Witt, J. (2015). Modeling Streamflow and Water Quality Sensitivity to Climate Change and Urban Development in 20 U.S. Watersheds. *Journal of the American Water Resources Association*, *51*(5), 1321–1341. https://doi.org/10.1111/1752-1688.12308

Karlsson, I. B., Sonnenborg, T. O., Refsgaard, J. C., Trolle, D., Børgesen, C. D., Olesen, J. E., … Jensen, K. H. (2016). Combined effects of climate models, hydrological model structures and land use scenarios on hydrological impacts of climate change. *Journal of Hydrology*, *535*, 301–317. https://doi.org/10.1016/j.jhydrol.2016.01.069

Kokkonen, T., Koivusalo, H., & Karvonen, T. (2001). A semi-distributed approach to rainfall-runoff modelling—a case study in a snow affected catchment. *Environmental Modelling & Software*, *16*(5), 481-493. doi: http://dx.doi.org/10.1016/S1364-8152(01)00028-7

Kuisi, A., Kuisi, M. Al, & El-naqa, A. (2013). *GIS based Spatial Groundwater Recharge estimation in the Jafr basin , Jordan – Application of WetSpass models for arid regions*.

Legrouri, B. A., Kettani, D., & Kalpakian, J. (2012). *Using Demand Side Management to Adapt to Water Scarcity and Climate Change in the Saïss Basin , Morocco*. (105439), 1–61.

Lewis, H. G., & Brown, M. (2001). A generalized confusion matrix for assessing area estimates from remotely sensed data. *International Journal of Remote Sensing*, *22*(16), 3223–3235. https://doi.org/10.1080/01431160152558332

Liew, M. W. Van, & Garbrecht, J. (2003). *Hydrologic Simulation Of The Little Washita River Experimental Watershed Using Swat 1*. *73036*, 413–426.

Lo, C. P., & Choi, J. (2004). *International Journal of Remote A hybrid approach to urban*

land use / cover mapping using Landsat 7 Enhanced Thematic Mapper Plus (ETM +) images. International Journal of remote Sensing, 25(14), 2687-2700. https://doi.org/10.1080/01431160310001618428

Loveland, T. R., Reed, B. C., Ohlen, D. O., Brown, J. F., Zhu, Z., Yang, L., & Merchant, J. W. (2000). Development of a global land cover characteristics database and IGBP DISCover from 1 km AVHRR data. *International Journal of Remote Sensing*, *21*(6–7), 1303–1330. https://doi.org/10.1080/014311600210191

Mccoll, C., & Aggett, G. (2007). *Land-use forecasting and hydrologic model integration for improved land-use decision support*. *84*, 494–512. https://doi.org/10.1016/j.jenvman.2006.06.023

Mishra, V. N., Rai, P. K., Kumar, P., & Prasad, R. (2016). Evaluation of land use/land cover classification accuracy using multi-resolution remote sensing images. *Forum Geografic*, *XV*(1), 45–53. https://doi.org/10.5775/fg.2016.137.i

Molle F.,Tanouti, O. (2017). *Squaring the circle : Agricultural intensification vs . water conservation in Morocco*. *192*, 170–179. https://doi.org/10.1016/j.agwat.2017.07.009

Moradkhani, H., & Sorooshian, S. (2008). General Review of Rainfall-Runoff Modeling: Model Calibration, Data Assimilation, and Uncertainty Analysis. In S. Sorooshian, K. L. Hsu, E. Coppola, B. Tomassetti, M. Verdecchia, & G. Visconti (Eds.), *Hydrological Modelling and the Water Cycle: Coupling the Atmospheric and Hydrological Models* (Vol. 63, pp. 12-35). Berlin: Springer-Verlag Berlin.

Moriasi, D. N., Arnold, J. G., Liew, M. W. Van, Bingner, R. L., Harmel, R. D., & Veith, T. L. (2007). *Model evaluation guidelines for systematic quantification of accuracy in watershed simulations*. *50*(3), 885–900.

Moradkhani, H., & Sorooshian, S. (2008). General Review of Rainfall-Runoff Modeling: Model Calibration, Data Assimilation, and Uncertainty Analysis. In S. Sorooshian, K. L. Hsu, E. Coppola, B. Tomassetti, M. Verdecchia, & G. Visconti (Eds.), *Hydrological Modelling and the Water Cycle: Coupling the Atmospheric and Hydrological Models* (Vol. 63, pp. 12-35). Berlin: Springer-Verlag Berlin.

Mukaya, M. (2017). *Simulation of land use changes and impacts on the water balance of an unconfined aquifer Case Study : Saiss Aquifer , Morocco. Master Thesis, FST-Fez, 100p.*

Neitsch, S.L.,Arnold,J.G.,Kiniry,J.R.,Williams,J.R.,&King, K. (2005). *Soil & Water Assessment Tool Theoretical Documentation Version 2005*.

Neitsch, S.L.,Arnold,J.G.,Kiniry,J.R.,Williams,J.R.,&King, K. . (2009). *Soil & Water Assessment Tool Theoretical Documentation Version 2009*.

Nolan, B. T., & Taber, P. E. (2007). *DigitalCommons @ University of Nebraska - Lincoln Factors influencing ground-water recharge in the eastern United States*.

Owuor, S. O., Guzha, A. C., Rufino, M. C., Pelster, D. E., & Breuer, L. (2016). Groundwater recharge rates and surface runoff response to land use and land cover changes in semi-arid environments. *Ecological Processes*. https://doi.org/10.1186/s13717-016-0060-6

Perrin, J. L., Raïs, N., Chahinian, N., Moulin, P., & Ijjaali, M. (2014). Water quality assessment of highly polluted rivers in a semi-arid Mediterranean zone Oued Fez and Sebou River (Morocco). *JOURNAL OF HYDROLOGY*, *510*, 26–34. https://doi.org/10.1016/j.jhydrol.2013.12.002

Reis, S. (2008). Analyzing land use/land cover changes using remote sensing and GIS in Rize, North-East Turkey. *Sensors*, *8*(10), 6188–6202. https://doi.org/10.3390/s8106188

Richards, J. A., & Jia, X. (n.d.). *Remote Sensing Digital Image Analysis*: An Introduction. https://doi.org/10.1007/978-3-642-30062-2

Rinsema, J. G. (2014). *Comparison of rainfall runoff models for the Florentine Catchment.* University of Tasmania. Retrieved from http://essay.utwente.nl/66526/1/Rinsema_Jan_Gert.pdf

Rwanga, S. S. (2013). *A Review on Groundwater Recharge Estimation Using Wetspass Model*. 156–160.

Santhi C., Arnold J. G, Williams J. R., Dugas W. A, Srinivasan R, and, H. L. M. (2001). *Validation of the Swat Model on a Large Riverr Basin with point and nonpoint sources. Journal of the American Water Resources Association*, *37*(5), 1169–1188.

Schilling, K. E., Jha, M. K., Zhang, Y., Gassman, P. W., & Wolter, C. F. (2008). *Impact of land use and land cover change on the water balance of a large agricultural watershed : Historical effects and future directions*. *44*, 1–12. https://doi.org/10.1029/2007WR006644

Shrestha, S., Bhatta, B., Shrestha, M., & Shrestha, P. K. (2018). Science of the Total Environment Integrated assessment of the climate and landuse change impact on hydrology and water quality in the Songkhram River Basin , Thailand. *Science of the Total Environment*, *643*, 1610–1622. https://doi.org/10.1016/j.scitotenv.2018.06.306

Singh, S. K., Laari, P. B., Mustak, Sk., Prashant, K. S., & Szabo, S. (2017). Modelling of land use land cover change using earth observation data-sets of Tons River Basin, Madhya Pradesh, India. *Geocarto International*, *33*(11), 1202–1222. https://doi.org/10.1080/10106049.2017.1343390

Tang, Z., Engel, B. A., Pijanowski, B. C., & Lim, K. J. (2005). Forecasting land use change and its environmental impact at a watershed scale. *Journal of Environmental Management*, *76*(1), 35–45. https://doi.org/10.1016/j.jenvman.2005.01.006

Tsarouchi, G.M., Mijic, A, Moulds, S and Buytaert, W. (2014). Historical and future land-cover changes in the Upper Ganges basin of India. *International Journal of Remote Sensing*, *35*(9), 3150–3176. https://doi.org/10.1080/01431161.2014.903352

Turkelboom, F., Poesen, J., & Trébuil, G. (2008). The multiple land degradation effects caused by land-use intensification in tropical steeplands: A catchment study from northern Thailand. *Catena*, *75*(1), 102–116. https://doi.org/10.1016/j.catena.2008.04.012

Uhlenbrook, S., Roser, S., & Tilch, N. (2004). Hydrological process representation at the meso-scale: the potential of a distributed, conceptual catchment model. *Journal of Hydrology*, *291*(3-4), 278-296. doi: 10.1016/j.jhydrol.2003.12.038

Venkateswarlu, Gogana, G Jayasankar, B. . S. (2014). Impact Assessment of Land Use Change on Ground Water Quality Using Remote Sensing & GIS for Zone V under Municipal Corporation Hyderabad. *IOSR Journal of Mechanical and Civil Engineering*, *11*(1), 36–42. https://doi.org/10.9790/1684-11153642

Warburton, M. L., Schulze, R. E., & Jewitt, G. P. W. (2010). Confirmation of ACRU model results for applications in land use and climate change studies. *Hydrology and Earth System Sciences*, *14*(12), 2399–2414. https://doi.org/10.5194/hess-14-2399-2010

Wijesekara, G. N., Gupta, A., Valeo, C., Hasbani, J. G., Qiao, Y., Delaney, P., & Marceau, D. J. (2012). Assessing the impact of future land-use changes on hydrological processes in the Elbow River watershed in southern Alberta, Canada. *Journal of Hydrology*, *412–*

413, 220–232. https://doi.org/10.1016/j.jhydrol.2011.04.018

Wilby RL (1997) Contemporary hydrology. John and Sons, England

Winchell, M. W., Rinivasan, R. S., & Uzio, M. D. I. L. (2013). *A RC SWAT I NTERFACE F OR SWAT2012 U SER ' S G UIDE*.

Yun, P. A. N., Huili, G., Demin, Z., Xiaojuan, L. I., & Nobukazu, N. (2011). *Impact of Land Use Change on Groundwater Recharge in Guishui River Basin , China*. *21*(41101033), 734–743. https://doi.org/10.1007/s11769-011-0508-7